Forecasting Research

Forecasting Research Division
Technical Report No. 118

Assimilation of AVHRR cloud top temperature - preliminary experiments.

by

N. Richards and R.S. Bell

September 1994

Meteorological Office
London Road
Bracknell
Berkshire
RG12 2SZ
United Kingdom

Forecasting Research Division
Technical Report No. 118

Assimilation of AVHRR cloud top temperature - preliminary experiments.

by

N. Richards and R.S. Bell

September 1994

1. Introduction

Cloud observations from satellites have been available for many years but have proved difficult to use in conventional data assimilation systems. There is an increasing desire to improve moisture analyses as the forecast model's parameterization schemes become more sophisticated and the expectations of the users of forecast products increases. CFO intervention forecasters have very crude facilities to generate bogus RH observations should they note substantial departures of model background RH fields from those deduced by 'eye-balling' a satellite image. The scheme described here attempts to provide a more sophisticated method of achieving their aim of a better match between model and observed cloud. In some sense it is a direct (albeit weaker) competitor to the MOPS system (Wright, 1993) currently used in the UM mesoscale assimilation, but the expectation is, that unlike MOPS, it can utilise satellite image data in mid-Ocean where no rainfall data or surface cloud reports are available to construct a complete vertical moisture profile. The cloud image data processing and the algorithm used for its assimilation is described in sections 2 and 3. A few impact study cases are presented in section 4 and some preliminary shortcomings are diagnosed. Section 5 deals with some enhancements to the scheme and a corresponding set of tests on the same initial data are performed. The impacts of this later version is compared to that of the first. Conclusions as to the performance of the scheme are made and suggestions for future upgrading are made.

2. Summary of the observation processing

The satellite observations used to obtain the assimilated cloud data are derived from the AVHRR instrument onboard the NOAA series of polar orbiting satellites. 5 channels are used, 3 visible and 2 infra-red, to derive a cloud top temperature image with all the clear sky pixels masked out. The first main processing stage is done on the UK MET Office Autosat-2 computer (deSilva,pers com) where Cloud-top temperature (CTT) histogram datasets are prepared (see section 2.1). These are routed via the HDS to the Cray where they are merged and reformatted (see section 2.2). to ACOBS format (Bell et al.,1993b). CTT histogram ACOBS files are available for use in the UK Met Office analyses correction scheme (Bell et al. 1993a) using a new vertical analysis (see sections 2.3 and 3).

2.1 Brief description of data (figure 1).

The data are in the form of cloud top temperature (CTT) histograms. A single histogram describes the distribution of cloud top temperatures for a particular model grid square as diagnosed from polar orbiting satellites. Only image pixels diagnosed as being completely cloudy are assigned a cloud top temperature. The clear sky pixel count is also supplied for each grid square because clearing unwanted model cloud is just as important as inserting cloud. The histogram values have been normalized to 256 so that a particular histogram band count is represented by a single byte integer. The sum of the histogram values does not

always add up to 256 however, as in practice some pixels are left undiagnosed. These 'undiagnosed' pixels remain when the cloud detection algorithm could not make a definite decision (deSilva, pers com).

There are seventeen 5° temperature bands ranging from 198°K to >283°K and one clear sky histogram band. Files are produced on Autosat-2 for each pass of the polar orbiting satellite with each file containing approximately 5000 histograms (one histogram per model grid box within the satellite swath)(Whyte et. al.,1993)

2.2 Processing the observations.

The files are copied from the Autosat-2 computer to a 24 hour rolling archive on the HDS. The data is in an Autosat-2 format [McCormack, pers com] and must be converted to ACOBS format for use by the UM. This is done by a routine, AC_HIST (Richards,1994), within the ACOBS program. It is hoped that all necessary quality control will be performed by Autosat-2 though at present this simply consists of the checks used in the algorithm to determine whether a pixel is cloudy or not. It is difficult to conceive of additional checks which could utilise model 'cloud' background fields.

The ACOBS program searches the 24 hour rolling archive of Autosat-2 formatted histogram datasets for observations with validity times between certain times on a particular date as specified in an input namelist. A single ACOBS file can therefore contain all CTT histogram observations for a whole assimilation run. Details of the namelist are appended at Annex A.

2.3 Overview of the Assimilation of the cloud top temperature histograms.

The general idea behind the assimilation of the cloud top temperature observations is to nudge the moisture variable RH in the model background towards values that will produce diagnosed cloud top temperatures similar to those observed from the satellite. The large scale cloud scheme in the model produces a direct correspondence between grid box averaged RH and the cloud cover, hence an estimation of cloud cover on a particular level made from an observation allows a corresponding estimation of relative humidity to be made. Of course the ice and liquid water contents of cloud layers covering 100% of the grid square cannot be estimated and so these variables are not directly adjusted during the assimilation though an indirect adjustment does occur in the following dynamical and physical steps. Heights are allocated to the observed cloud tops by searching the model profile for matching temperature levels.

As with other observation types, the calculation of increments at each model grid point is achieved first by interpolating model to observation, first horizontally then vertically. The (observation - background) differences are then spread in the vertical according to vertical error correlation coefficients and then spread horizontally using the filtered increment scheme which lends itself well to the analysis of high density observation fields. Due to the high density and resolution of the observations in the horizontal the influence of a particular

observation is not permitted to spread much horizontally. The horizontal spreading scale used is 100km. More details of the vertical processing algorithm are provided in the next section.

3 Details of the Assimilation Algorithm

3.1 The vertical analysis

The observation data passed to the new vertical analysis routine 'VANCLD' contains the cloud top temperature histogram and clear sky pixel count for each model grid square under the satellite swathe. No information concerning errors is passed in with the data. (Values are hardwired at present , see section 3.6). The background relative humidity and potential temperature are also passed to the routine.

The vertical analysis takes place in two stages

1. Produce a column of observation - background increments and vertically spread these increments.

2. Multiply the increments by a weight determined by the observation density and correlation scale.

3.2 Creation of model profile,interpolation and conversion from θ to T

For each model time step during the assimilation cycle a background temperature and relative humidity profile is produced for each observation position. First the model background relative humidity and potential temperature are interpolated to the observation position. The EXNER function (P/100000.) $^{\kappa}$ and the surface pressure are also interpolated to enable the θ to T conversion. Since the observations are at model grid points horizontal interpolation could be avoided. Unfortunately this short cut could not easily be taken because of the use of latitude and longitude to define observation position rather than model grid point location. Though there is obviously some wasted calculation taking place, this method will allow the same histogram data to be assimilated using different model resolutions.

From the model profiles, tropopause heights are calculated (using the UM tropopause modelling scheme) for each observation point. This is to allow for a check to ensure that no moisture is inserted into the model stratosphere.

3.3 Adjustment for cloud occultation (figure 2).

Cloud amounts are adjusted on each temperature band to give a presumed actual cloud fraction on a layer and not simply observed cloud fraction. [A simplifying assumption that there is a linear relationship between temperature and height is made thus warmer cloud top implies lower cloud.] Cloud in this scheme is assumed to overlap randomly between layers. Adjustment of this part of the scheme will play a part in future experiments.

The formula giving the 'diagnosed' cloud cover for a particular layer j is given below.

$$Cover_j = \frac{C_j}{D - \Sigma_{i=N..j+1} C_i}$$

Where C_i is the satellite observed cover for level i and N is the number of model wet layers. D is the proportion of 'diagnosed' pixels within the grid square. By diagnosed it is meant those pixels for which the algorithm for determining whether an observation is cloudy or clear (referred to in section 2.1) has made a definite decision. There are some pixels for which the algorithm makes no decision as to whether a brightness temperature is that of a cloud top or the ground. The denominator on the right hand side represents the 'observable fraction' of the grid square while the numerator is the 'cloudy fraction' of the grid square observed with a range cloud top temperature lying within the histogram band ranges denoted by the index j.

3.4 Assignment of model levels to histogram temperature bands (figure 3)

For each cloudy histogram temperature band at each observation position the model levels are searched from the tropopause to level 2 for a model temperature within the temperature band width of the observed cloud layer. Cloud is not inserted into level 1 as early tests of the scheme showed that excessive cloud was being inserted into the lowest layer.

In an attempt to assimilate cloud into levels where the model is likely to retain cloud, the scheme tests adjoining model levels for higher relative humidity levels and will insert the cloud into the level with the higher RH. The scheme will only make this test if the observation is cloudy and the model level initially chosen is clear.

Observed cloud layers where the proportion of observed cloudy pixels falls below a critical level of the total pixels are not used. For initial tests this has been set to one sixteenth of grid square cover.

There is in theory a danger that the above method could allocate non adjacent model levels to adjacent temperature bands. In other words cloud which when observed appears to be continuous in the vertical could sometimes be assimilated to separated model levels. It is hoped the vertical spreading of increments will alleviate this problem. Also this problem is only likely to occur when lapse rates are low or when the vertical resolution of the model is increased. Neither will this algorithm cater for cloud under inversions by allocating the highest model temperature level. In practice however model levels are rarely exceed a temperature difference of 5^0 and inversions are rarely resolved sufficiently to allocate a correct temperature level below an inversion. This will change with increased vertical resolution and a future experiment will include techniques of inserting cloud under inversions.

3.5 Allocation of fractional cloud cover to the model levels

A fractional cloud cover is allocated to model levels which have been allocated to a cloudy observation. The fractional cloud cover is the layer observed fractional cover as diagnosed by the method described in section 3.3. Sometimes one model level will be allocated to more than one observed cloud top temperature fraction. In this case a maximum is chosen. An addition is not made due to the complexity of getting this code to run efficiently. It is hoped that this situation does not occur frequently enough to impact the assimilation significantly.

3.6 Assigning an RH to the model levels according to cloudiness, the calculation of the RH increment and the errors applied for the AC scheme.

All cloudy diagnosed levels are given an RH based on the inverse of the function used to calculate cloudiness on a model level in the large scale cloud scheme [ref UM doc 29].

By inverting equation P292.19 from UM doc 29 we obtain the relation

$$RH = RH_{crit} + \frac{\sqrt{2C}[3-C](1-RH_{crit})}{3}$$

This equation is used when $C<0.5$ where C is cloud cover diagnosed on a model level and RH_{crit} is the critical relative humidity at which cloud in the model begins to form.
For $0.5<C<1.0$ we invert equation P292.21 to obtain

$$RH = 1-(1-C^{\frac{3}{2}})\frac{\sqrt{2}}{3}(1-RH_{crit})$$

An RH increment profile can then be calculated. A value for the ratio of observation plus representivity error variance to background error variance $(\varepsilon_o^2/\varepsilon_b^2)$ must also be supplied. There are 4 case where an observational increment can be determined and each has been assigned a different $(\varepsilon_o^2/\varepsilon_b^2)$. They are listed below.

1. A cloudy observation and a cloud free background RH

$(\varepsilon_o^2/\varepsilon_b^2) = 0.25$

Here the derived RH from the relative humidity is likely to be more accurate than the background relative humidity simply because we can observe cloud.

2. A cloud-free observation but a cloudy background field.

$(\varepsilon_o^2/\varepsilon_b^2)$ =1.0

A cloud-free observation is allocated to those model levels which for which there is a signifcant proportion of grid square observable from the satellite but for which no cloud tops are observed (ie. the level is not obscured by colder and therefore higher cloud). In this case a significant proportion is 1/4 or more of the grid square. This figure is somewhat arbitrary as there is no obvious technique of determining what an appropriate value should actually be.

Here no RH has actually been derived but we can assume that the RH humidity is below $RH_{crit.}$ The increment used is $(RH_{crit}\text{-}10.0)\text{-}RH_{background}$. Of course 10% below RH_{crit} is a rather arbitrary value to move toward, but it is better to aim to remove the incorrect cloud than to worry about the uncertainties of the RH values in the cloud free observation. During the assimilation the background will eventually become cloud free at just below RH_{crit} and case 4 will apply.

3. Cloudy observation and cloudy background.

$(\varepsilon_o^2/\varepsilon_b^2)$ =1.0

Here it has been decided to give equal weighting to the model and the derived RH. The error variance ratio should be more than in case 1 because we have more faith in the background field.

4. Cloud-free observation and background.

$(\varepsilon_o^2/\varepsilon_b^2)$ =4.0

In this situation the observation can only infer that the model is probably correct in having a relative humidity below $RH_{critical}$. The scheme assigns a zero increment with a low level of confidence hence $(\varepsilon_o^2/\varepsilon_b^2)$ is high.

Cloud-free observations are only diagnosed for temperature layers for which a significant proportion of the grid square (arbitrarily taken to be 1/4) is found to be visible from the satellite using the algorithm as described in section 3.3. For layers in the model where there is no diagnosed cloud observation (clear or cloud-free missing) data indicators are inserted. It is recognised that the values of $(\varepsilon_o^2/\varepsilon_b^2)$ chosen are somewhat arbitrary but it was not clear how a more objective approach to their specification could be taken.

The algorithm produces an incomplete column of (o-b) RH increments. The levels which are undetermined, being obscured by near complete cover of higher cloud, are assigned a zero increment and a missing data indicator for the error variance ratio. The incomplete columns are passed to the vertical spreading routine VRTF, which fills in the missing levels by

interpolation from near neighbours. In this way a complete column of RH increments is produced wih coresponding $(\varepsilon_o^2/\varepsilon_b^2)$ values

3.7 Observation density and weights.

This second part to the vertical analyses is performed in exactly the same way as is for radiosonde relative humidity (Bell 1993a) though the weights derived using the observation density are calculated using a much smaller radius of influence and cut off than for radiosonde data.

3.8 Summary of the vertical analyses

Figure 4 shows a summary of 3.1-3.6. the left hand third of the chart shows the CTT histogram plotted on the same axes as the model temperature profile. Grey lines then show how each cloudy histogram band is mapped to a model level. The model levels are represented by the horizontal black dashed lines. The second third of the diagram shows the vertical humidity profiles of both the model background and that which has been derived from the histogram observations. The thin grey line running vertically denotes the critical RH above which cloud forms. Note that the derived 'observed profile' clears the highest cloud increases the mid level cloud and dries out the low level cloud. The last third of the diagram shows the accuracy given to each increment as assigned via the $(\varepsilon_o^2/\varepsilon_b^2)$ error variance ratio.

4 Case studies.

Four cases have been examined from the month of May 1994. These cases (from 1st, 3rd, 11th and 22nd) were chosen as they present a variety of weather regimes. Figure 5 shows the midday analyses for each case.

For each case an initial two sets of runs were performed. The first was a control 12 hour morning assimilation (with no input of CTT histogram data) followed by a 12 hour forecast and the second corresponding run with the CTT histogram data. This first version of the algorithm we shall refer to as VANCLD#1. In this paper T+0 is the analysis time after a 12 hour assimilation. T-6 refers to a time during the assimilation cycle 6 hours before the final analysis time.

4.1 12z Analyses

We concentrate on the cloud analyses and model derived precipitation analyses. Before discussing the analyses, several things should be noted. Firstly, both the control and test runs were based on UM version 3.3 with the additional modification to prevent radiosonde humidities from drying the analysis (Bell, 1994). Secondly, the comparison between observed cloud and model cloud fields is not ideal, the former being displayed as cloud top and the latter as cloud amount. For this reason our conclusions are backed up be height cross-sections

in the later discussion. Thirdly, in the morning period the satellite overpass times usually fall well before 12GMT. On the 1st May, the overpass times were 5:07, 6:48, 8:45 and 10:26 GMT. This means that the conventional data (over land) valid at 12GMT will have a much more significant impact on that analysis from which the forecast is run.

4.1.1 May 1st case

The plot of the total histogram coverage is shown in figure 6, grey scale co-ordinated to show the coldest significant cloud layer in each grid square. 10% cover is deemed to be significant. Each plot corresponds to the data accumulated in the 12 hour assimilation period and where grid squares have satellite observations of two or more satellite passes the earliest observation is plotted. Above the chart a histogram is shown from a random location. The white areas correspond to grid boxes diagnosed as being clear or containing an insufficient number of diagnosed pixels with which to make a decision (<1/5 coverage). An inspection of the data revealed that a significant proportion of the white areas come under the second category of being undiagnosed. These undiagnosed pixels tend to occur over North Africa and are likely to correspond to clear skies. If there is a bias in that most undiagnosed pixels are indeed clear then this may be leading to problems in determining cloud cover.

Comparisons of the noon T+0 cloud amount and associated precipitation rate analyses are shown in figures 7(a-d). The cloud fields (7a,b) are those used by the long wave radiation scheme which uses a random overlap between non concatenated layers and a maximum overlap between adjacent layers. The precipitation rates (7c,d) are convective and large-scale combined. The left most charts (7a,c) relate to the control and the rightmost charts (7b,d) are the VANCLD#1 run.

The VANCLD#1 run tends to spread cloud over a greater area but reduces the amount of dense cloud, ie. total cloud coverage tends to be greater as averaged over the whole area of coverage. Comparing figures 7a and 7b, for example, the VANCLD#1 analysis has large areas of partial coverage over the Atlantic Ocean not apparent in the control run. This finding is supported by an earlier climate study, the results from which are appended (annex B). The region of complete cloud cover is reduced as can be seen by a comparison of the same charts in the cloud band to the north and west of the British Isles stretching up to Greenland . This implies that there would be less precipitating cloud in the VANCLD#1 run. An inspection of the precipitation rate charts (figure 7c and 7d) shows that this is indeed the case for the band of rain associated with the same area of cloud along the front indicated in figure 5a. We suspect that this reduction in complete coverage in frontal areas is probably unrealistic, although the cloud top observations (figure 6) show considerable non-uniformity (in terms of the grey scale) both in this frontal area and also the front over north Germany where cloud is also reduced.

The increase in total cloud coverage is made of contributions to sea stratus, which is more predominant early in the assimilation cycle (T-6) as can be seen in figure 8. Compare control charts (far left, 8a,d) with the VANCLD#1 run charts (centre, 8b,e) for total cloud

and precipitation rates at 6GMT; (The far right charts are for the VANCLD#2 tuning run and will be discussed in a later section). The satellite CTT observations (figure 6) shows large areas stratus over the Atlantic and North Sea which matches reasonably well with the cloud assimilated in the same regions, both at T-6 (figure 8b) and T+0 (figure 7b). We should note, however that the additional stratus produces areas of precipitation (eg off the Norwegian coast in figure 8e), which might be overdone.

Another effect of the VANCLD#1 run is to enhance convective activity, especially over land. Again this is clearer to see at T-6, since by T+0 the additional radiosondes and absence of cloud observations at that time result in the analyses converging. This can be seen from the rainfall analyses (figure 8e compared with 8d). Though these combine large scale precipitation with convective, it was determined that the precipitation over land was largely from the convective parameterisation. The insertion of observed cloud over land is probably enhancing convective activity over land to an unrealistic level.

4.1.2 May 3rd case

Figures 9 and 10 show the respective cloud observations and model cloud, rain analyses for this second case (with the same format as for the first case (figures 6 and 7). In most cases where frontal precipitation is apparent the VANCLD#1 runs reduce greatly (or if not completely dry out) the rain rate associated. This is the best case from those chosen to examine the effects of frontal rain rates due to the positioning of a frontal rain band lying across the UK from Northern Ireland to Wales. Figure 11 shows a Frontiers generated radar rain rate analyses for noon for comparison with the charts shown in figure 10c,d. The VANCLD#1 run (figure 10d) has incorrectly dried out this rain band compared to the control run (figure 10c) where it is present, albeit further west.

4.1.3 May 11th case

Figures 12 and 13 show the respective cloud observations and model cloud, rain analyses for this third case (with the same format as for the first case (figures 6 and 7). In this case the same general thinning of the clouds takes place and again the associated rainfall has been lost in some areas (notably near Iceland and the frontal rain band stretching from Ireland to the Bay of Biscay). Cloud amounts, a few degrees to the west of Ireland are reduced in the VANCLD#1 run in accordance with the clear skies observed in figure 7c.

4.1.4 May 22nd case

Figures 14 and 15 show the respective cloud observations and model cloud, rain analyses for this last case. Again, the impact of the CTT histogram assimilation has been to reduce cloud amounts as can be seen over the Atlantic, British Isles and the North Sea. The precipitation apparent over the NE of England and the North sea is almost completely dried out. In this case cloud has been poorly assimilated in the region just to the south of Iceland. The observations suggest a large area of clear skies, whereas both the control and assimilation runs

contain large areas of stratus in the same regions. It is unclear as of yet why the assimilation has failed in these areas and this case will be examined further at a future date. This case does highlight the difficulty associated with assimilating low cloud.

4.2 Forecast results.

Here we concentrate on the first two cases. Figure 16 shows the T+12 cloud and rain comparison for May 1st (in our standard format), with validation of the rain field at Figure 18a. Figure 17 gives the same forecast plots for 3rd May to be compared with the validation in figure 18b.

Though greatly reduced in magnitude, similar differences to those noted in the comparison of analyses are observed inn the forecast comparison. It would also appear that impact on cloud does not last as long as it does on the precipitation rates.

For the first case, the precipitation forecast seems to be poor for both runs with regard the rain band through the Irish Sea, though the control run does have the showers represented better over Ireland.

For the second case, the VANCLD#1 run seems to have captured the orographically enhanced rain on the west coast of Scotland slightly better than the control run. It also has correctly reduced the rain to the southwest. There is a very large difference in dynamical rain rate over the Bay of Biscay in that the VANCLD#1 run has forecast an area of very heavy precipitation. This is difficult to verify and coastal reports and later synoptic observations do not support this forecast rain. This very large impact on the forecast precipitation rate needs further investigation.

4.3 Discussion

To determine more precisely where the problems might lie, figures 19 shows cross sections of cloud fraction for noon 1st May through a frontal region of cloud at 6z. Figure 8 (far left and centre charts) shows the 6z (T-6) cloud and precipitation charts for the same period. Care must be taken when visualising the cross sections as a line on the cloud, precipitation and frontiers charts. The latitudes and longitudes are given for each cross section and are slightly different for the two cases but both approximately lie (from left to right) from a point off the South west of Ireland (50N,15W), just past the tip off the NW coast of Ireland, over NW Scotland and the North sea to points lying very close to the NW coast of Norway (70N,10E). Figure 20 shows a selection of histograms from the satellite data the bottom two of which lie along the line of the cross section.

The middle histogram is an observation of the cloud top temperatures of the sea stratus in the northern North Sea. This cloud has been successfully inserted but is precipitating near the Norwegian coast (This rain cannot be verified and does not last even until 12z). The lowest

histogram corresponds to the higher cloud south and west of Ireland. This cloud is thinned during the assimilation cycle. The coverage represented in each of the adjoining temperature bands is always less than 50%. Even with the compensation in the vertical analysis algorithm for randomly overlapping cloud layers layer cloud fraction on the model levels is reduced. Again the algorithm has performed as expected. In this particular case there is no precipitation from frontal cloud.

The case for the 3rd of May (cloud amount cross sections are shown in figure 21) contains a frontal rain band (800 km from left axis). The frontiers precipitation analyses was given in figure 11. Figure 10 showed that this precipitation band was dried out by the VANCLD#1 run. Figure 22 shows a selection of histograms from the assimilated CTT data. The upper two histograms correspond to observation in the precipitating band (800 km from left axis in cross section) while the lowest corresponds to the area of low stratus to the north eastern end of the cross section. Again it would appear that no level in the precipitating band of cloud is observed to have complete cloud cover as is seen in the control run (top cross section in figure 21). The observed reduced cloud amounts have been successfully assimilated in the VANCLD#1 run and the precipitation is completely dried out.

5. Tuning Experiments.

5.1 Doubling up of temperature layers

In tests (described in the above section) it was evident that this scheme greatly reduced the amount of precipitation from frontal bands. This could have been due to a horizontal displacement between the model front and the observed frontal cloud band but on closer inspection it was found that the RH derived for actual cloud cover for the deep precipitating frontal cloud observed was not high enough to produce model precipitation. This at first seems to suggest problems with the model cloud scheme. To remedy this cloud fraction for a particular layer was derived by concatenating adjacent cloudy temperature layers in the histogram to produce a higher cloud fraction in the model than actually observed to allow the precipitation scheme to generate more convincing rain rates in frontal regions.

5.2 Reduction of influence of observations overland.

Earlier runs also suggested that too much cloud was being diagnosed over land in the imagery leading to the exaggerated convective activity. We considered that for the satellite observations over land, less faith should be given to the diagnosed cloud amounts because a) other sources of data are available and b) there is more scope for confusion with the land surface in the retrieval algorithm. For this reason $(\varepsilon_o^2/\varepsilon_b^2)$ is increased 5 fold for cloudy observations over land. For a cloudy observation and cloudy background, $(\varepsilon_o^2/\varepsilon_b^2)$ =5.0 is used and for a cloudy observation with a cloud free background, $(\varepsilon_o^2/\varepsilon_b^2)$ =1.25 is used.

5.3 Version 2 of the Vertical cloud analyses.

The changes to the vertical analyses algorithm outlined above were made and a new routine VANCLD#2 created. The four cases were rerun. For brevity, we only discuss the first two cases.

5.4 Results

Charts of 12z analyses and 12 hour forecasts for the 1st are shown in figure 23. Corresponding charts for the 3rd are shown in figure 24. There is a definite improvement in the frontal rain patterns in the VANCLD#2 runs in both cases compared with VANCLD#1.

For the first case, the relevant comparisons are between figure 23a,c and figure 7 for the analyses and between figure 23b,d and figure 16 for the forecast. In the VANCLD#1 analysis, much of the rain 'lost' from the front in the Atlantic has been restored. The forecast is also more correctly like the control, both being slow but having more rain than VANCLD#1.

For the second case we compare figure 24a,c with figure 10 at analysis time and figure24b,d with figure 17 at forecast time. Again the frontal rain at analysis time has been restored, but still seems deficient compared with the control when compared with the validation shown at figure 11. The forecast remains on a par with that from VANCLD#1, which was deemed to be better than the control except for the erroneous feature in Biscay.

Unfortunately, the effect of reducing the weight of low level cloud insertion over land seems to be outweighed by the effect of doubling up the cloud layers and the problem associated with convective cloud and precipitation activity has been aggravated rather than solved. We refer back to the rightmost charts of figure 8 which show that VANCLD#2 does not compare well with the earlier runs in this respect. The increased convective activity is evident over Southern France and Northern Italy. There are also increased precipitation rates over mid Atlantic and off the coast of Norway.

Figure 25 shows cloud fraction cross sections. The top cross section is for the 1st of May and the lower for the 3rd of May (comparable with those in figures 19 and 21 respectively). There is a thickening of cloud on most levels compared to the VANCLD#1 run thus allowing the precipitation scheme in the model to diagnose rain in the frontal regions An examination of the sea stratus (1st May case) shows that the sea stratus is also enhanced in the new run producing more areas of unverifiable rain early in the assimilation period (see figure 8f) which does not last until the analysis time of 12z (see figure 23d). We suspect that the different textures of the tops of deep frontal cloud and lower flatter non-frontal clouds are the root cause of the above problems

6 Conclusions.

Cloud can be successfully assimilated in the form of relative humidity increments to produce realistic cloud amounts and that the cloud formations themselves verify reasonably well with the satellite observations. The coverage of the satellite data mean that the cloud analyses are greatly improved over areas of the oceans where conventional observations are scarce.

The main problem with the assimilation of cloud into the NWP model is that the apparently more realistic cloud amounts tend to produce unrealistic precipitation rates.

It seems to be 'unsafe' to assimilate low cloud. Low cloud in the model with 100% cloud cover is allowed to precipitate. This precipitation does not last long into the forecast but nevertheless is undesirable. Better retention of this sea stratus may be achieved by not necessarily allowing this cloud to precipitate but for the time being it would be preferable not to insert cloud at all in the lower levels. Drying out low cloud in the NWP where clear skies are observed in the model should remain an important aspect of the algorithm.

Recommendations for future changes to the vertical analyses are therefore only to insert higher cloud with a doubling up of the cloud layers to allow cloud amounts to be assimilated in frontal regions which are sufficient to allow precipitation to continue.

An algorithm to detect convective cloud should be included though using model convection may be preferable to trying to detect convection by analysing grid-box CTT histograms.

7. References

Wright, BJ, 1993, 'Evaluation of the Automated Version of the Moisture Observation Pre-processing System (AutoMOPS), FR Tech Rep No 79

Whyte, KW,1993, 'Investigation into the use of AVHRR Imagery in Numerical Weather Prediction Data Assimilation' , 6th AVHRR Data Users' meeting, Belgirate, Italy.

Bell, RS et al 1993a, 'The Analysis Correction Data Assimilation Scheme' UMDP 30

Bell, RS et al 1993b, 'Technical Details Of the Unified Model Data Assimilation Scheme' UMDP P3

Bell, RS, 1994, "Moisture spinup - a possible solution", FR tech Rep No 90

Richards, NR, 1994, 'AC_HIST ,Creating acobs files from Autosat-2' , access via FR HP mosaic system - personal home pages.

Smith, R.N.B et al. 1990, 'Calculation of Saturated Specific Humidity and Large Scale Cloud', UMDP 29

Appendix A - ACOBS Namelists.

The main body and namelists used in the ACOBS program are already documented [ref. G.Bason 1994]. The additions to namelist ACOBSF are two variables ACLEN and N_HISTS.

N_HISTS	The number of raw histogram AUTOSAT2 files to be read in. The AUTOSAT-2 files must be assigned to unit numbers 70 and upwards.
ACLEN	The length of the time window, starting from yy,mm,dd,hh, in hours of the observations to be selected for this acobs file.

When copying the autosat-2 data from the HDS to the CRAY, df=tb must be used on the getibm.

Appendix B - A climate study.

An experiment to investigate model biases using monthly mean analyses.

Here satellite CTT data is collected and archived for a whole month (May 1994). The May 1994 mean monthly cloud cover climatology is derived (at present only for the morning orbits, figure B1).

A control mean cloud cover derived from model analyses (without CTT observations) is given for comparison (figure B2). The CTT histogram observations are also assimilated throughout the month and a comparable mean monthly cloud cover model analysis for the same period is derived (figure B3). Both these mean fields are based on a mean of the 12GMT analyses only.

Figure B4 shows a chart of the number of histogram observations per grid square in the month. Note the deficiency in observations at the margins of the field. For this reason, we examined only a small area of the LAM in detail. The test-control cloud cover difference for this area is shown in figure B5.

Mean Cloud Cover Patterns

The model climatology derived using the cloud observations is clearly closer to the observations than the control. On charts B1,B2,B3 the 80% average cloud cover contour is highlighted with a dark line to make comparisons easier. The histogram assimilation cloud climatology (figure B3) shows that areas of high average cloud cover ,above 80%, are much more widespread than in the control run (figure B2). This higher level of average cloudiness is verified in the observation climatology shown in figure (B1). This trend is predominantly evident over the Atlantic though is observed over the whole chart area including Europe. An inspection of chart B5, the test-control cloud difference chart, shows that the highest increases in average cloud cover are in fact over land.

Mean cloud and relative humidity biases

Average total cloud cover is increased from 55% in the control run to 68% in the histogram assimilation analyses. The observation diagnosed May cloud cover is 74%. We can infer from this that the satellite observed cloud is being assimilated producing a positive impact on the analyses. Using this as evidence of a beneficial analysis we can go on to take a look at cloud on different levels. The tables below shows the impact of the CTT assimilation on cloud for three layers and relative humidity at four levels. The results shown below suggest that the model diagnoses too much high cloud and not enough low cloud with the overall cloud cover being too low. The relative humidity is diagnosed as being too high in all levels but especially

lower levels. The possibility of a +ve bias in high cloud and a -ve bias in relative humidity can be explained by the fact that when the scheme dries out cloud it only reduces the background relative humidity to a level marginally below the critical cloud forming value thus resulting in large areas of high humidity but zero cloud content grid boxes.

The biases in relative humidity could either be due to genuinely low RH fields or due to deficiencies in the large scale cloud scheme

Cloud

Layer	Control	CTT analyses	Difference
High	23%	16%	7%
Medium	20%	29%	-9%
Low	26%	39%	-13%

TABLE 1 : AREA MEAN, TIME AVERAGED CLOUD AMOUNTS - MAY 1994

RH

Level	Control	CTT analyses	Difference
950mb	69%	74%	- 5%
850mb	60%	66.5%	- 6.5%
700mb	50.6%	57.5%	- 6.9%
300mb	49%	51%	- 2%

TABLE 2 : AREA MEAN, TIME AVERAGED RELATIVE HUMIDITY - MAY 1994

Fig 1 . The data

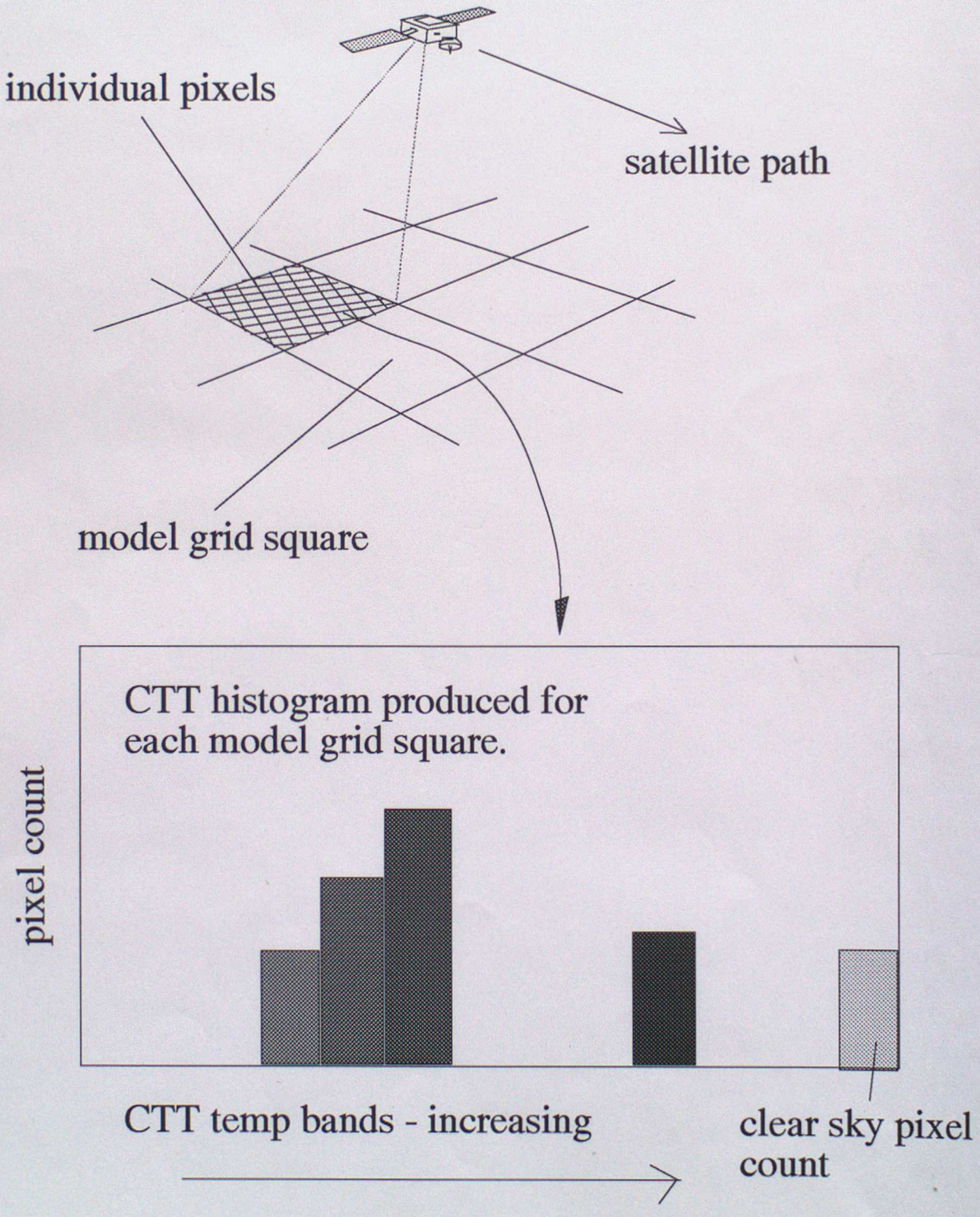

Fig 2. diagnosed cloud cover on temperature levels as diagnosed assuming random overlap with higher cloud.

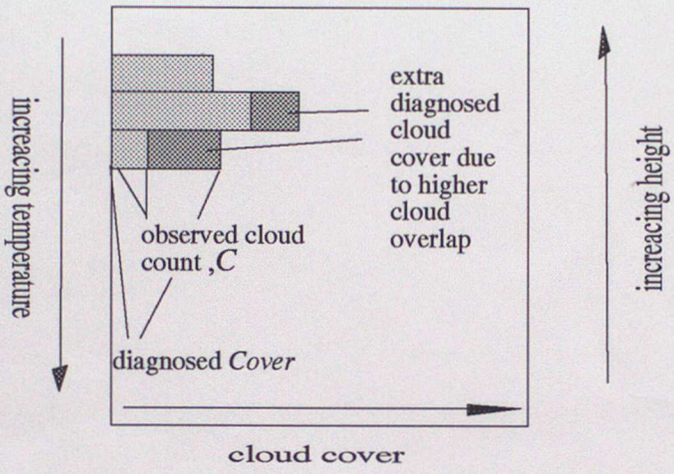

fig 3. Each cloud layer is associated with a single model layer.

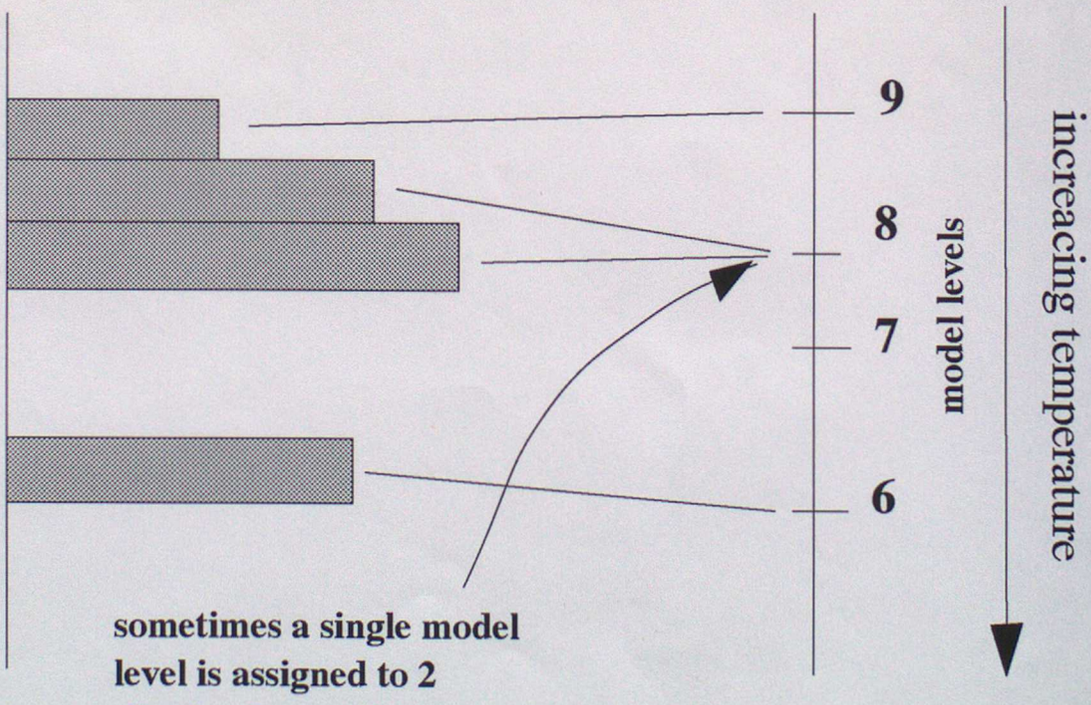

fig 4. Resulting increments from a given histogram.

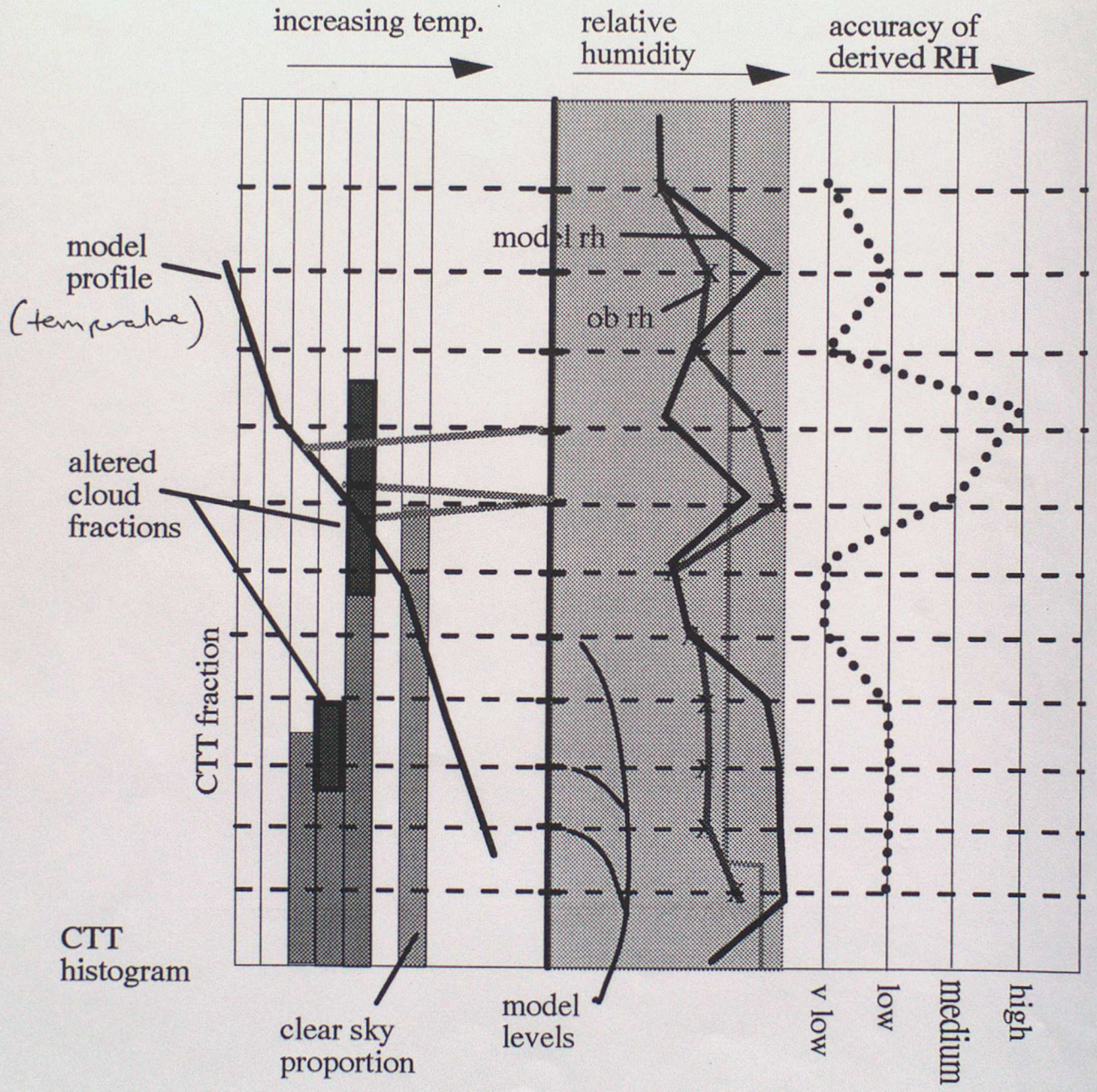

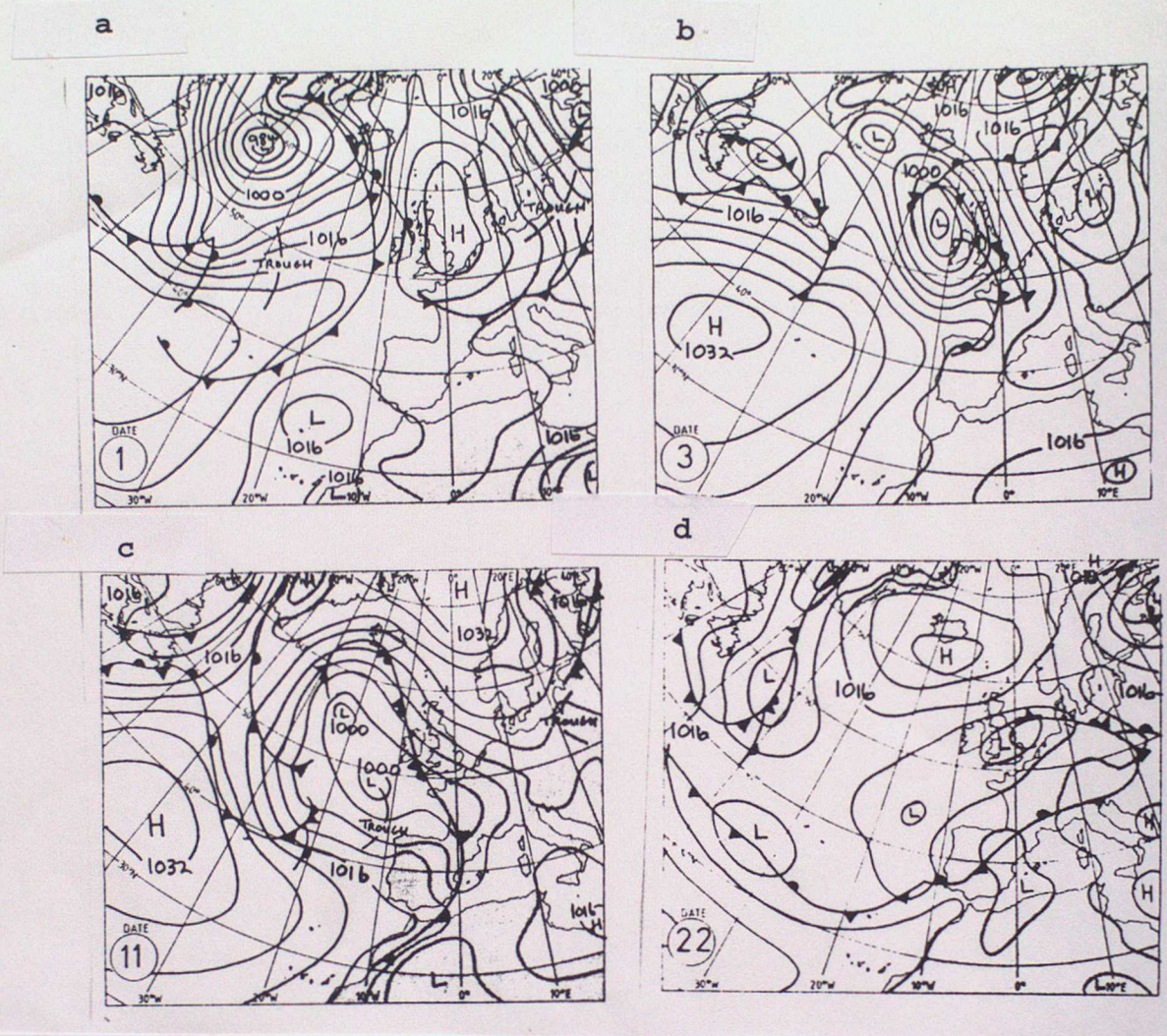

Figure 5.
The noon analyses (from Weather magazine) for the 4 days of may taken as test cases.

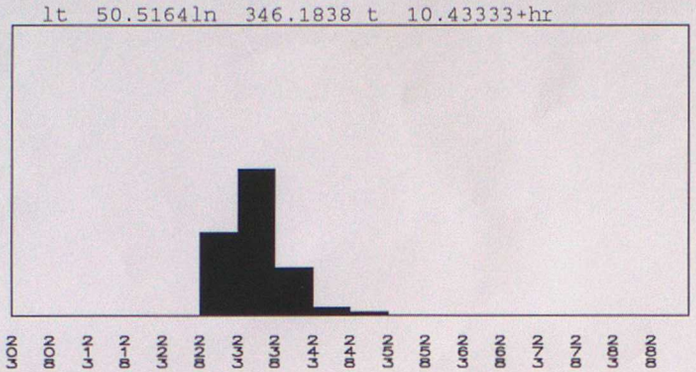

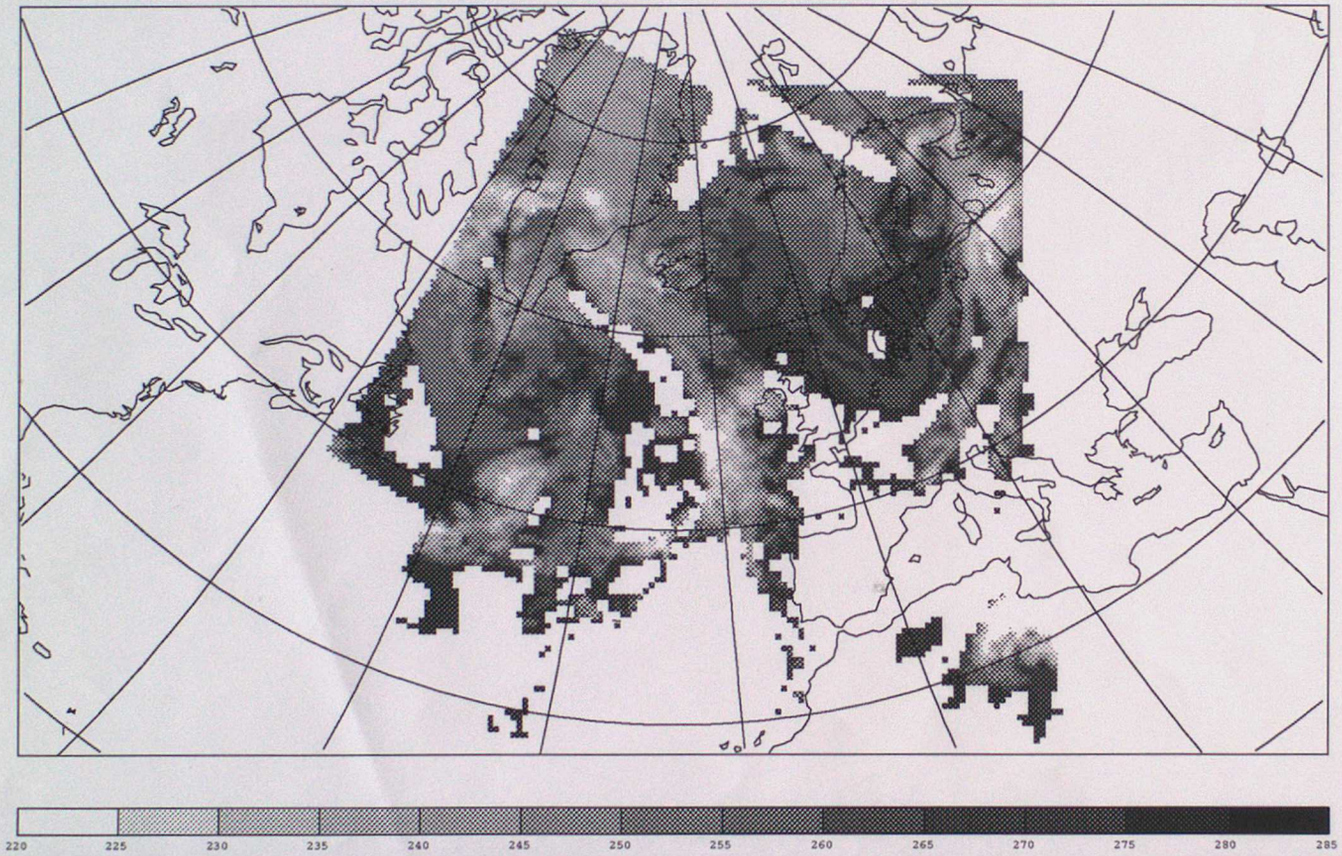

Figure 6

Plot of observation coverage for the 1st May. Each pixel coloured to earliest satellite observation and coolest observed significant cloud coverage. White areas inside satellite swathes correspond to areas of undiagnosed data (over the Sahara)or diagnosed clear skies. The image contains 4 Swathes timed a t 5:07 , 6:48 , 8:45 and 10:26 and compose of around 28,000 histograms. The histogram above shows a randomly selected example histogram from the data. the right most bar is reserved for clear sky pixels.

a control assimilation

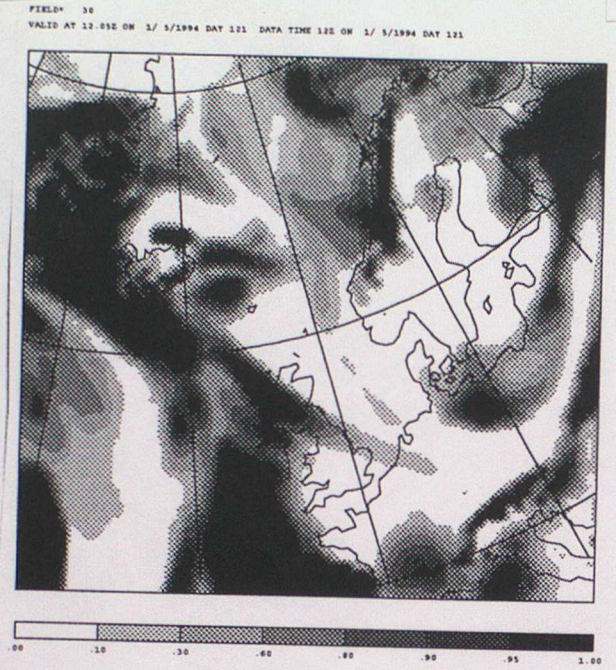

b VANCLD#1

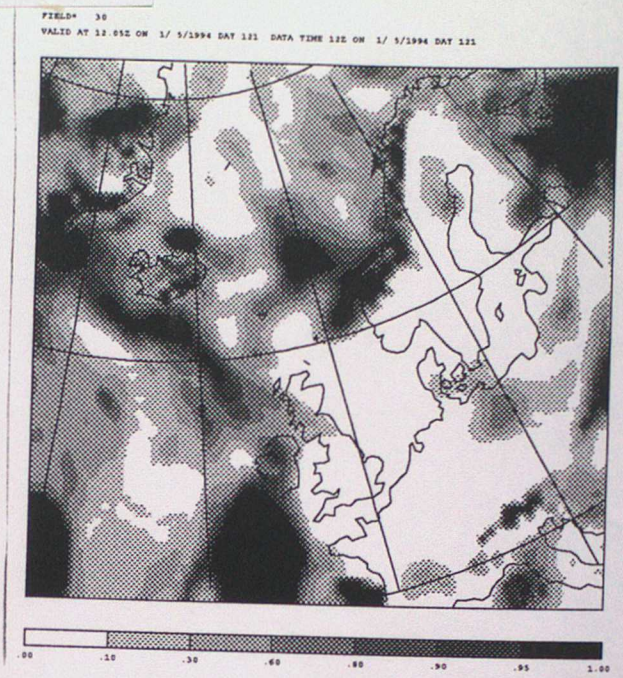

c

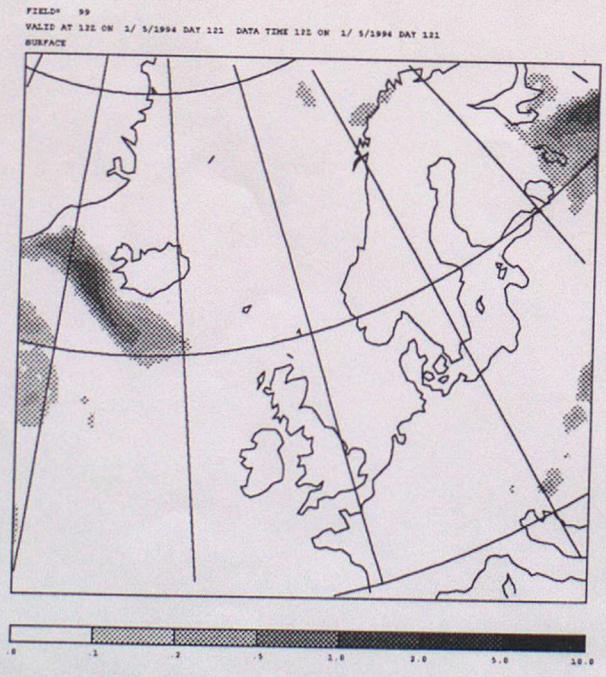

d

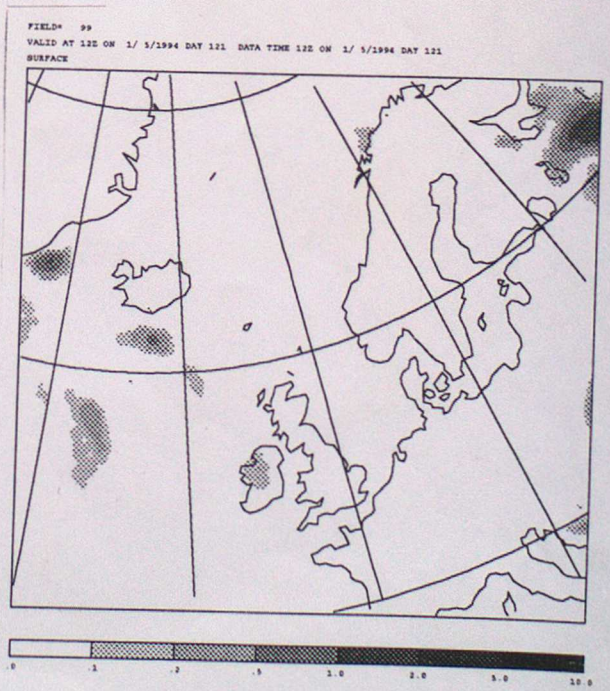

Figure 7a-d

The 12z analyses for May 1st showing total cloud cover and precipitation rates for both control assimilation and VANCLD#1 runs.

control assimilation

VANCLD#1

VANCLD#2

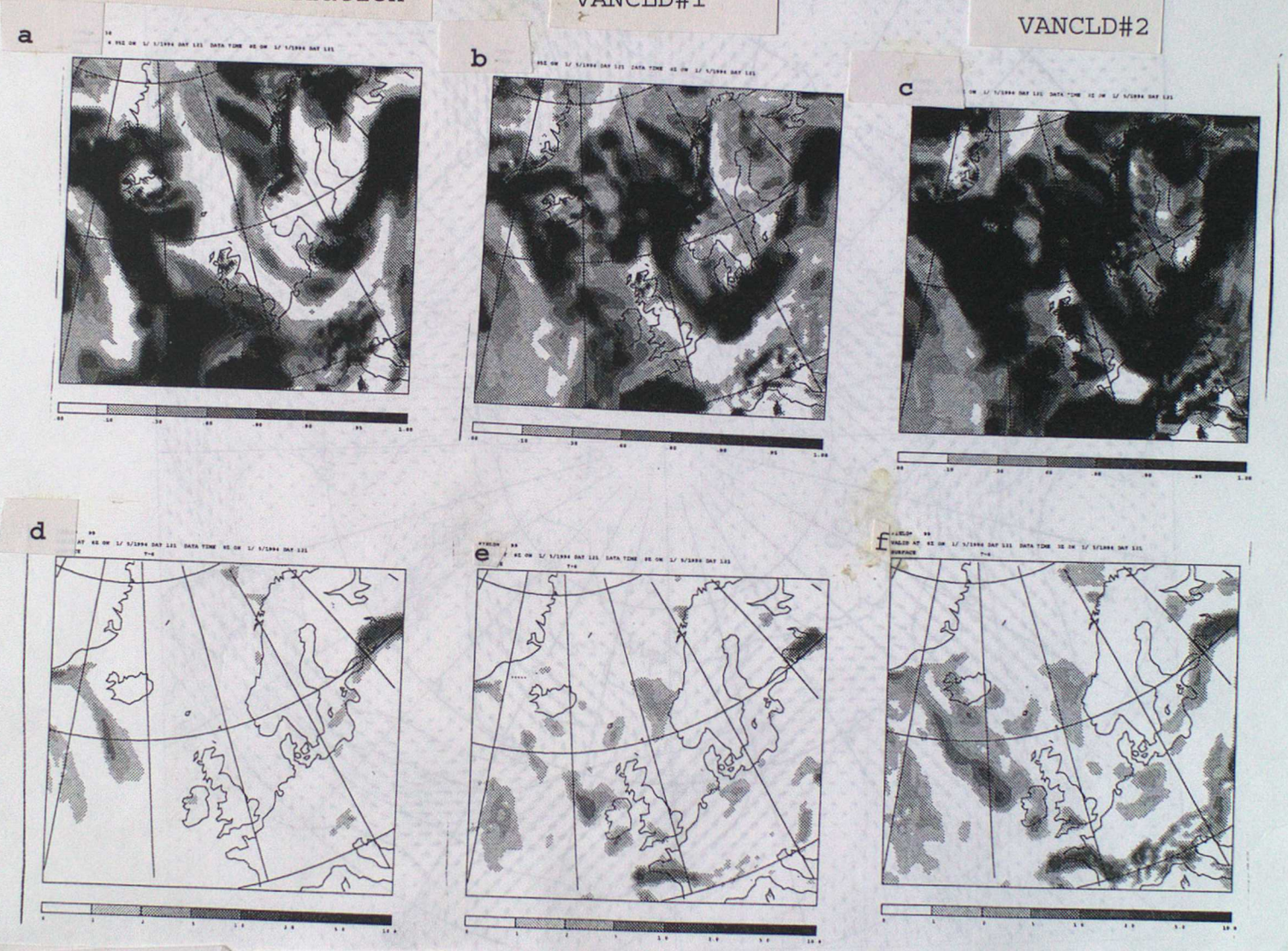

Figure 8a-f
6z charts for 1st May showing cloud and precipitation for all 3 assimilation runs - control , VANCLD#1 and VANCLD#2 from top to bottom.

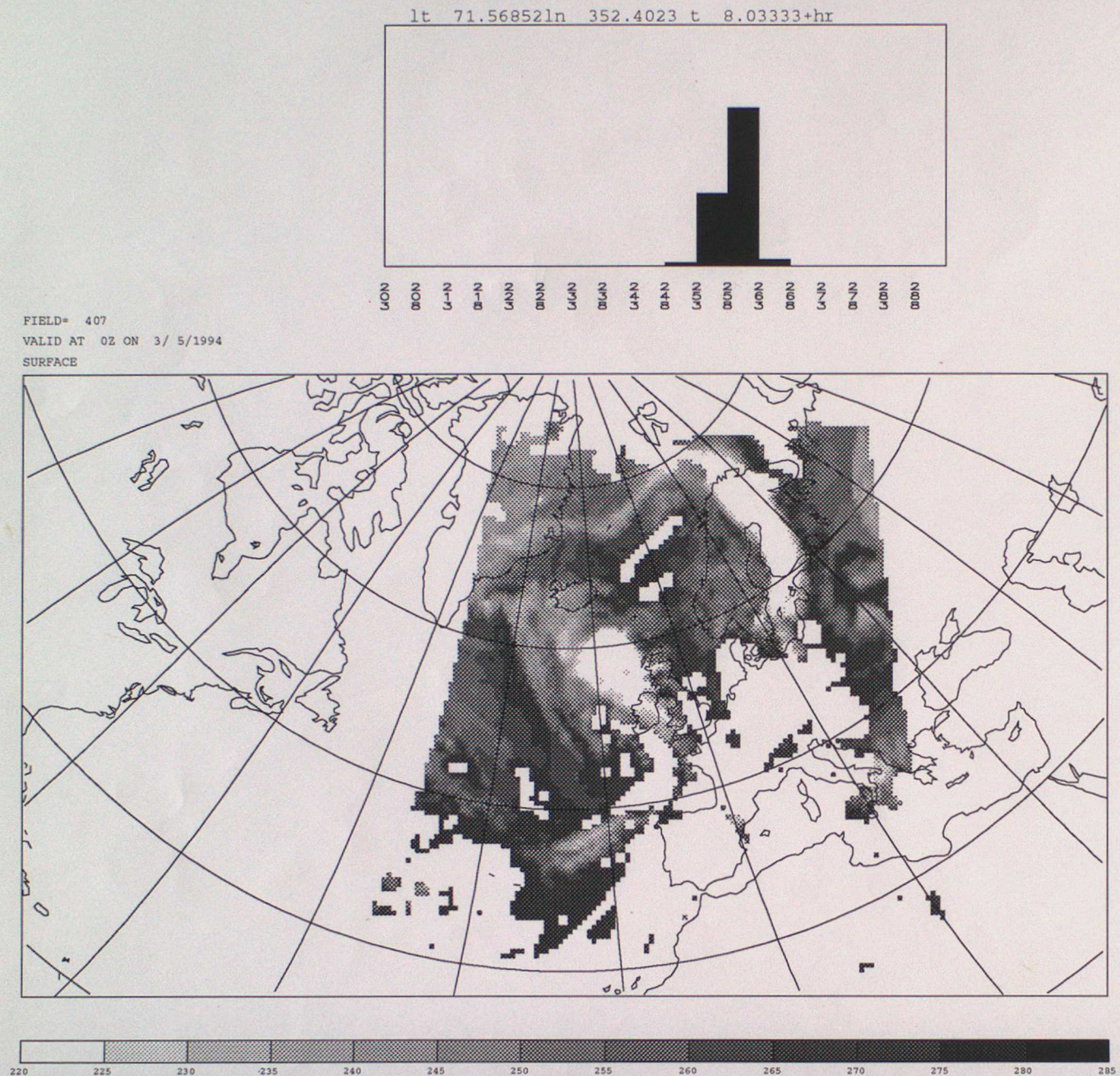

Figure 9
as for 6 but for May 3rd.

control assimilation

VANCLD#1

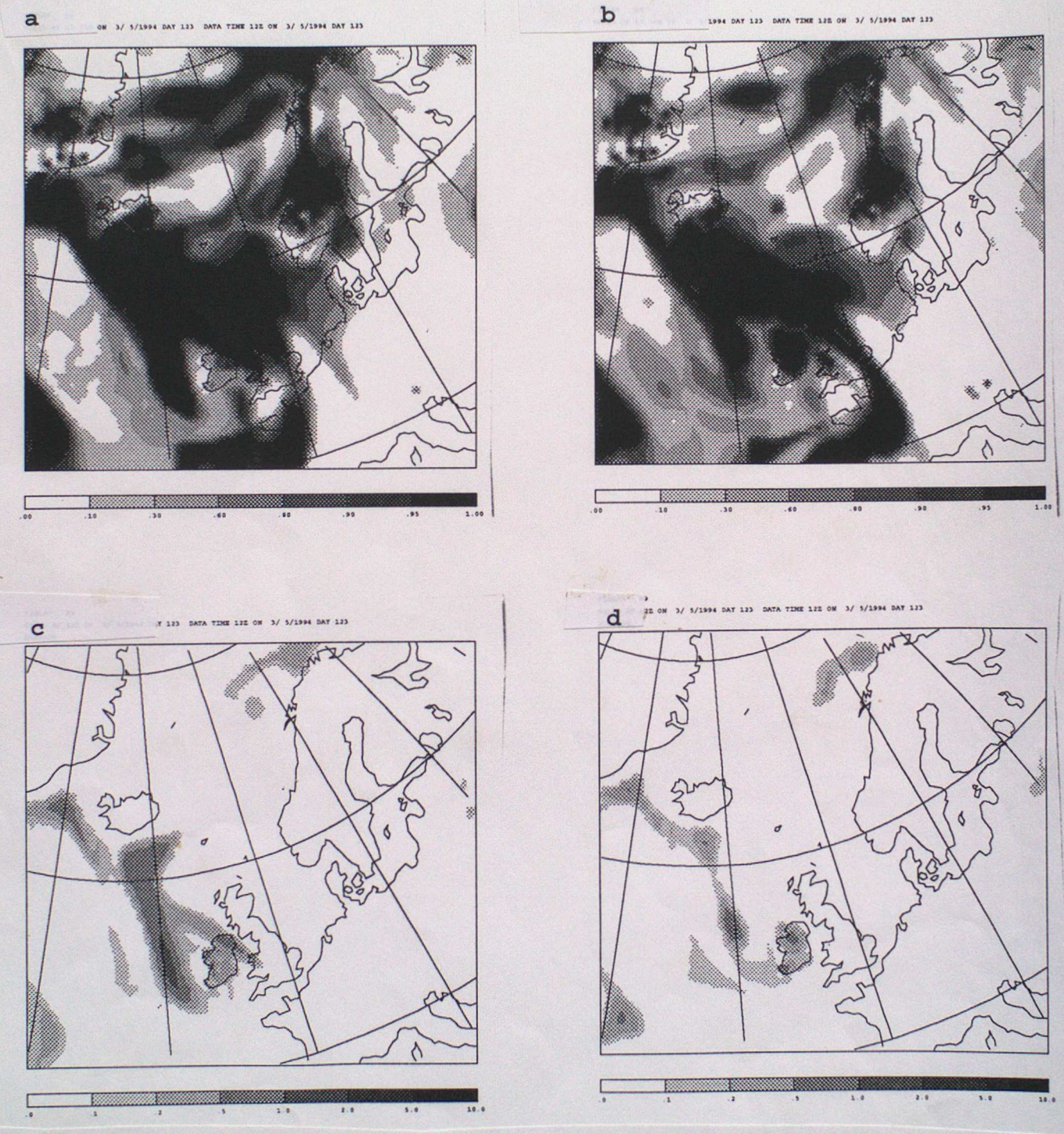

Figure 10a-d
The 12z analyses for May 3rd showing total cloud cover and precipitation rates for both control assimilation and VANCLD#1 runs.

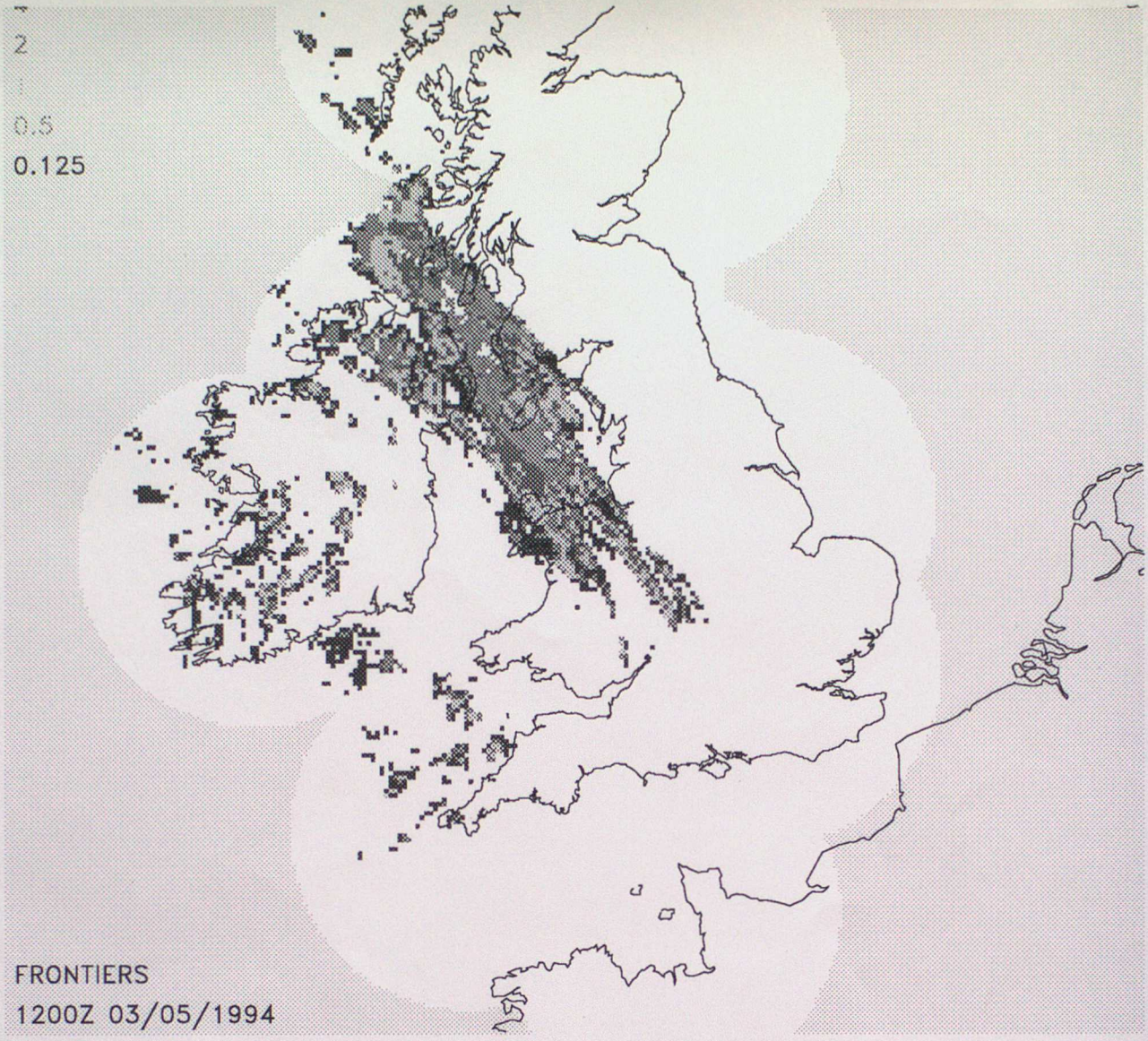

Figure 11
Frontiers data for the 3rd of May (noon) for use in verification. This was the only significant band of rain across the British isles from the cases chosen.

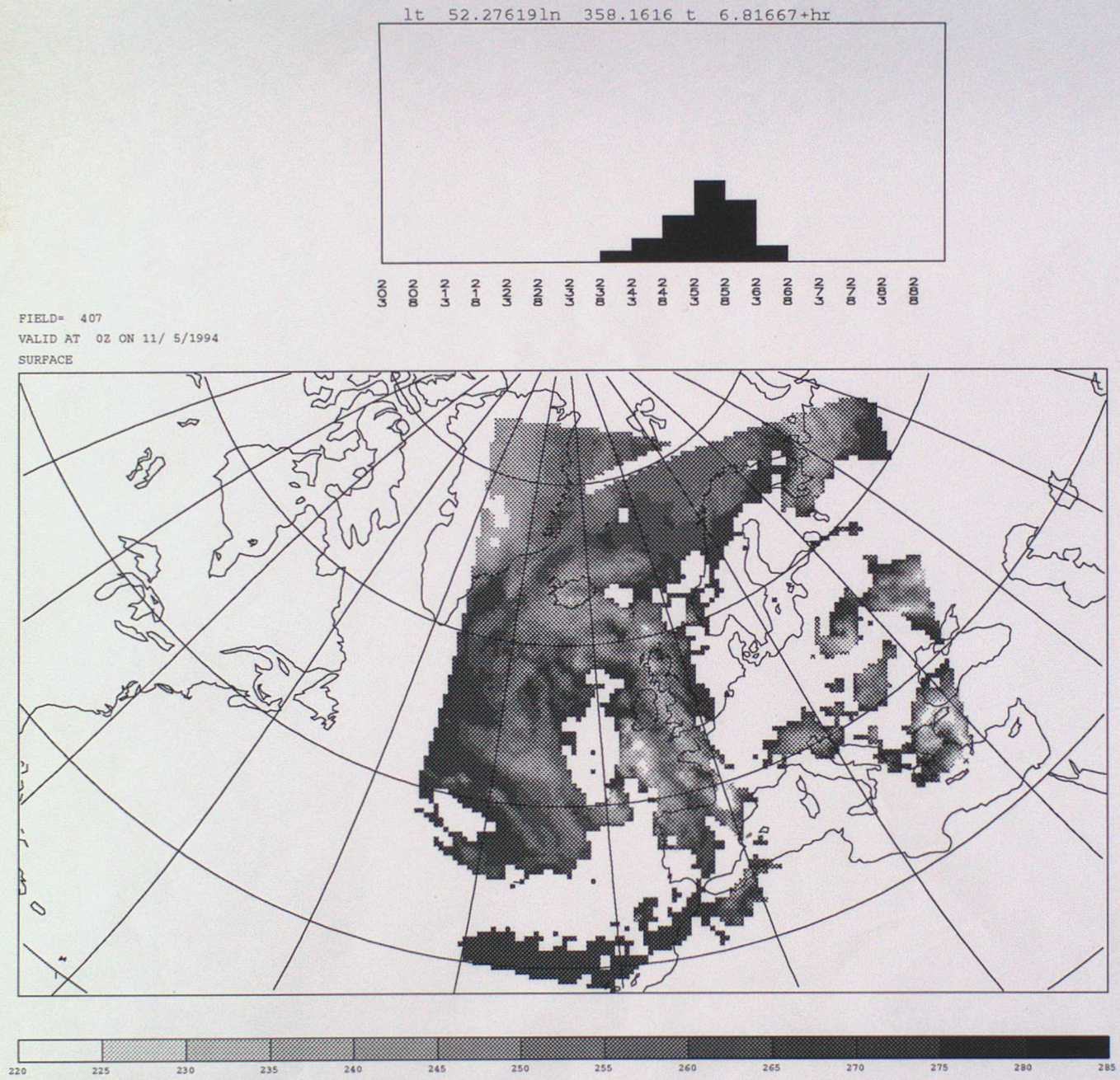

Figure 12.
as for 6 but for May 11th.

control assimilation

VANCLD#1

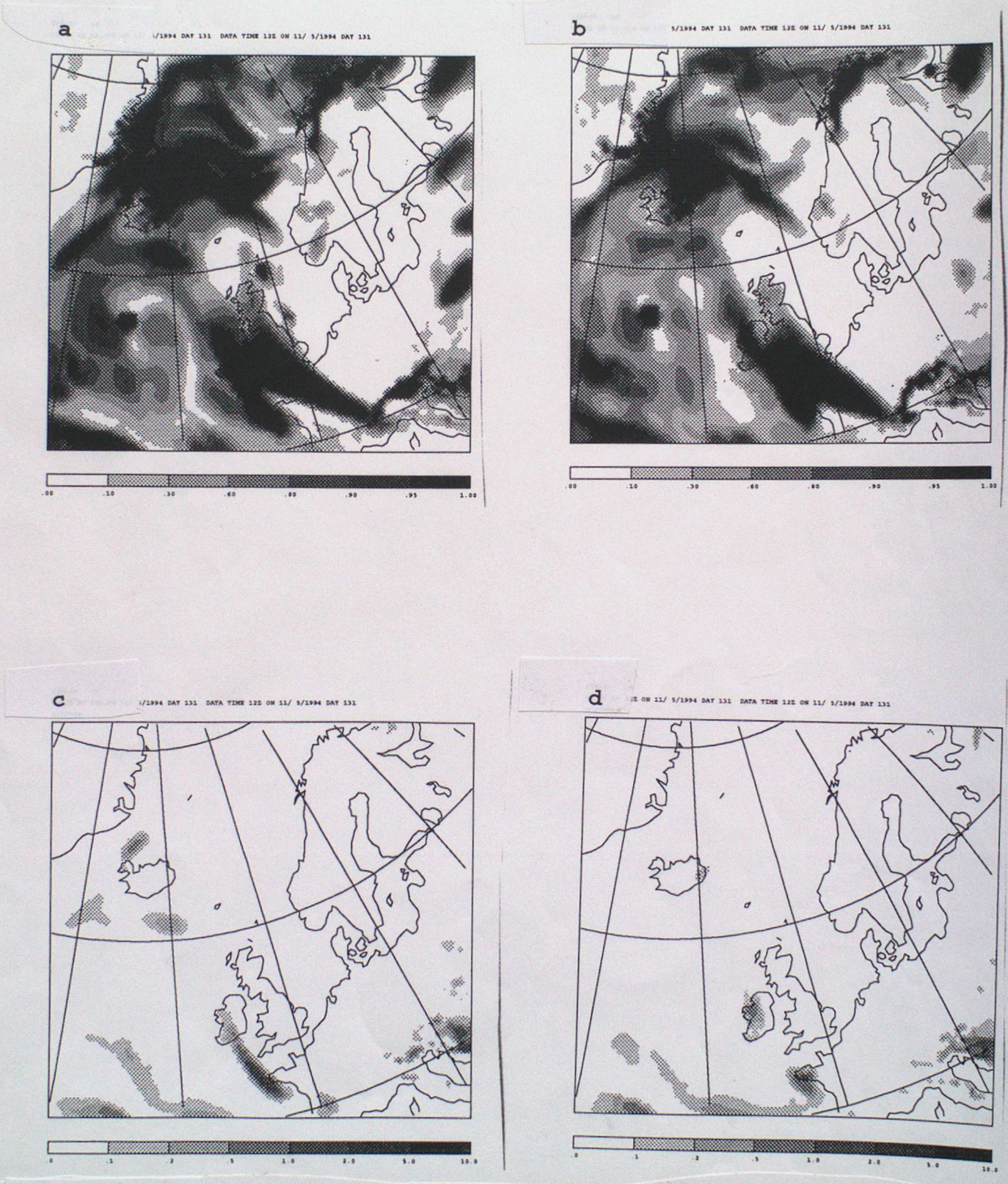

Figure 13a-d
The 12z analyses for May 11th showing total cloud cover and precipitation rates for both control assimilation and VANCLD#1 runs.

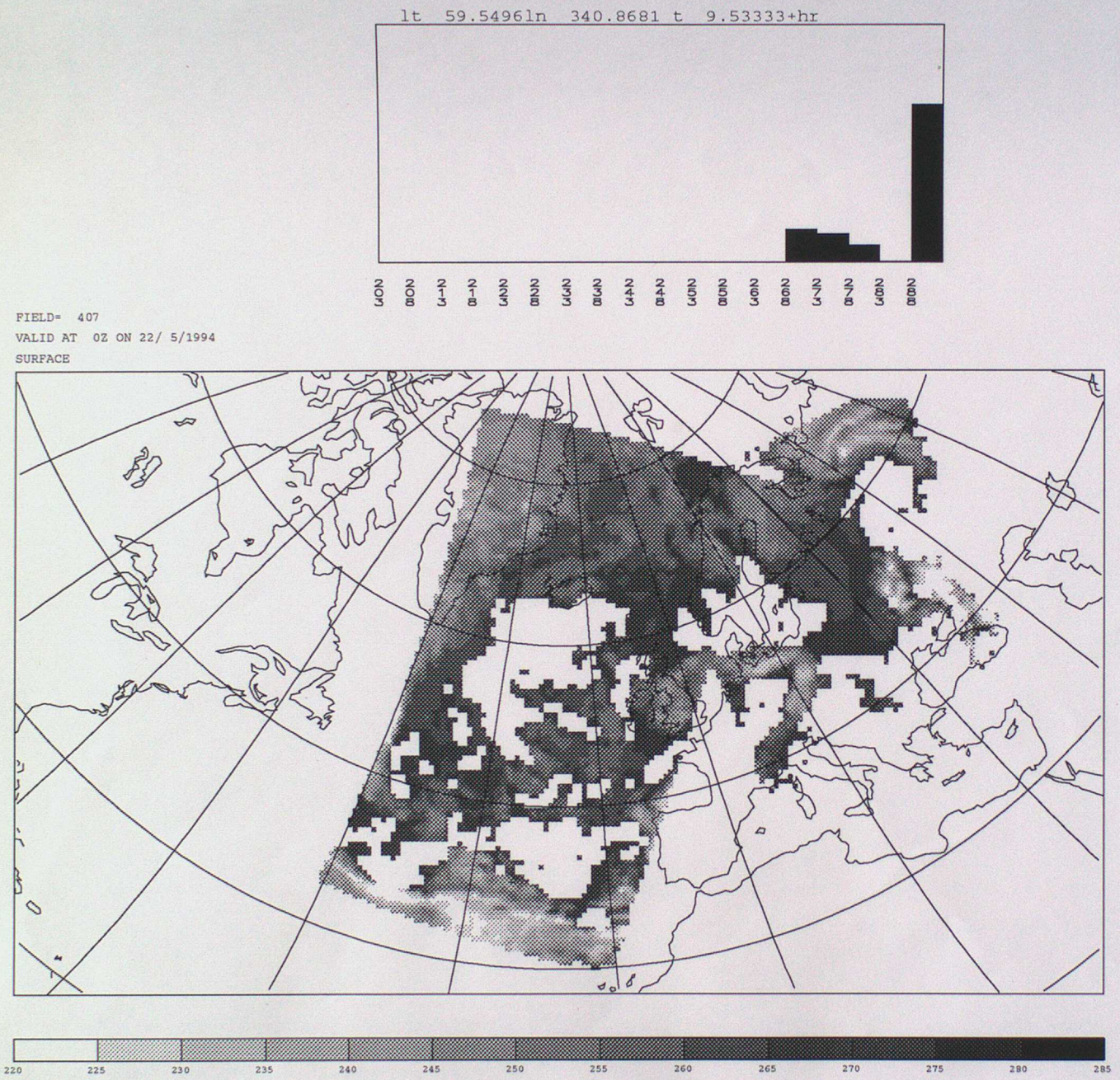

Figure 14.
as for 6 but for May 22nd.

control assimilation

VANCLD#1

Figure 15a-d
The 12z analyses for May 22nd showing total cloud cover and precipitation rates for both control assimilation and VANCLD#1 runs.

control assimilation

VANCLD#1

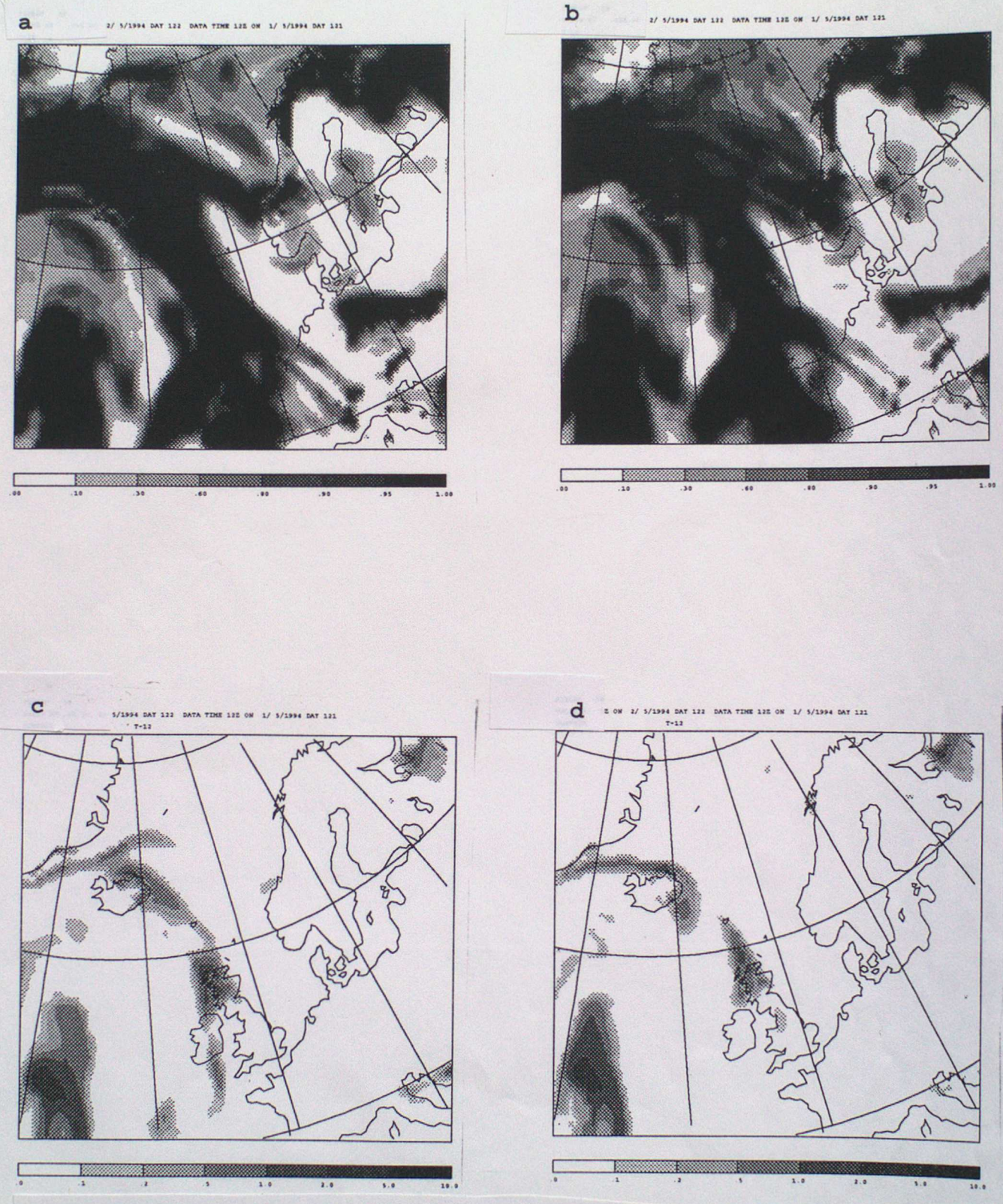

Figure 16a-d
The 12hr forecasts for May 1st showing total cloud cover and precipitation rates for both control assimilation and VANCLD#1 runs.

control assimilation

VANCLD#1

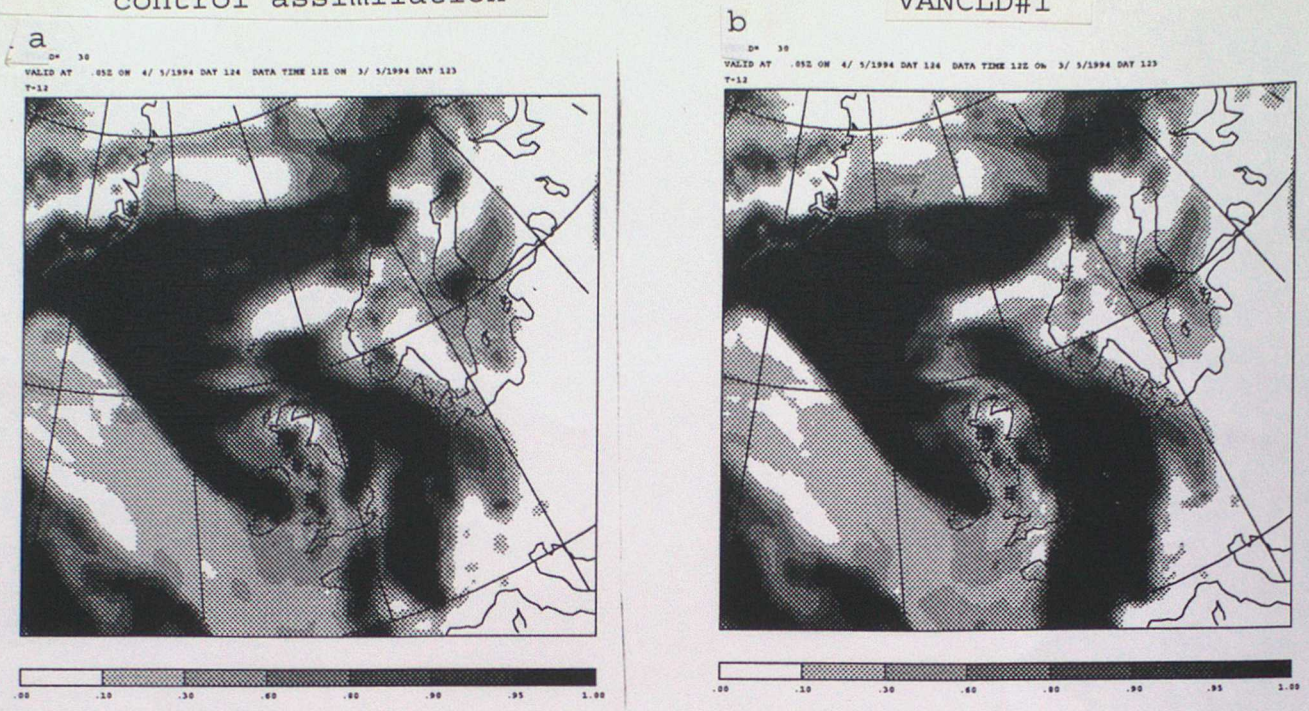

Figure 17a-d

The 12hr forecasts for May 3rd showing total cloud cover and precipitation rates for both control assimilation and VANCLD#1 runs.

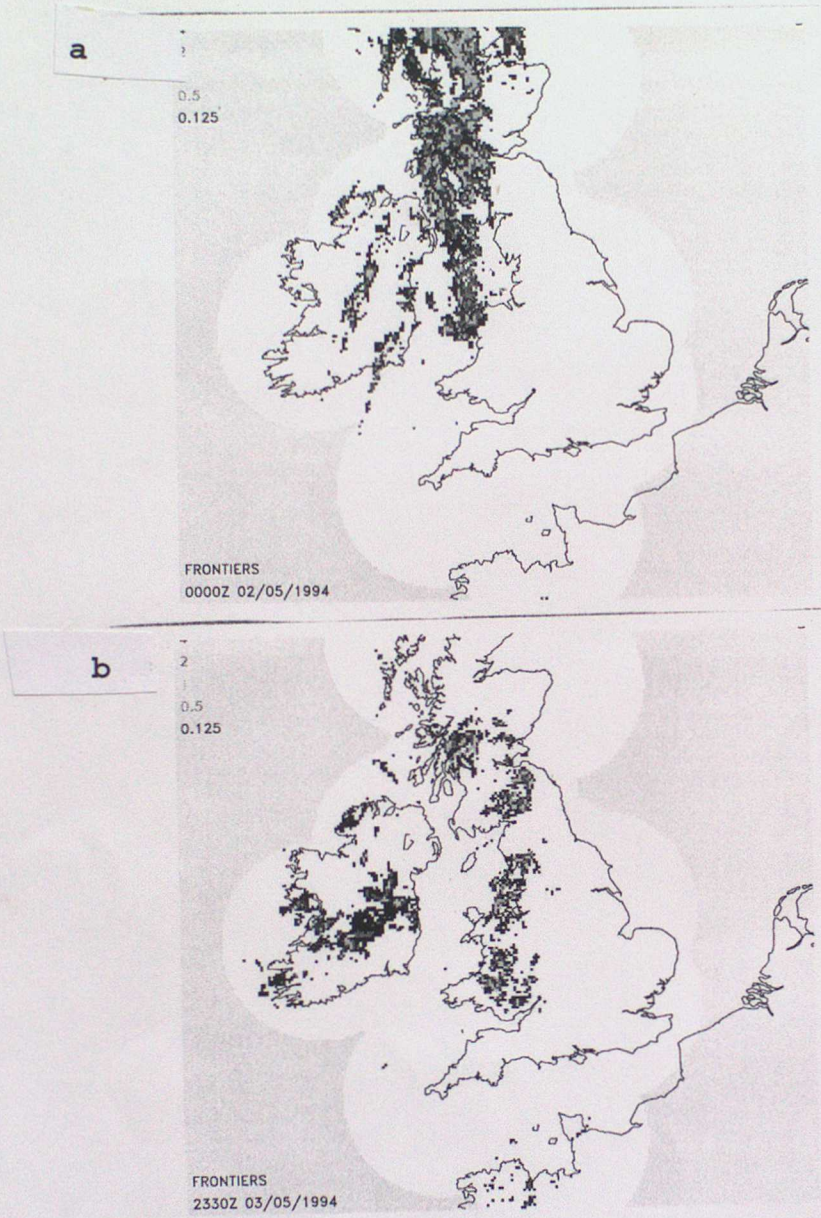

Figure 18a-b
Frontiers rainfall analyses for the UK area for 0000Z on the 2nd and 2330Z on the 3rd of May for comparison with figures 10a and 10b.

a

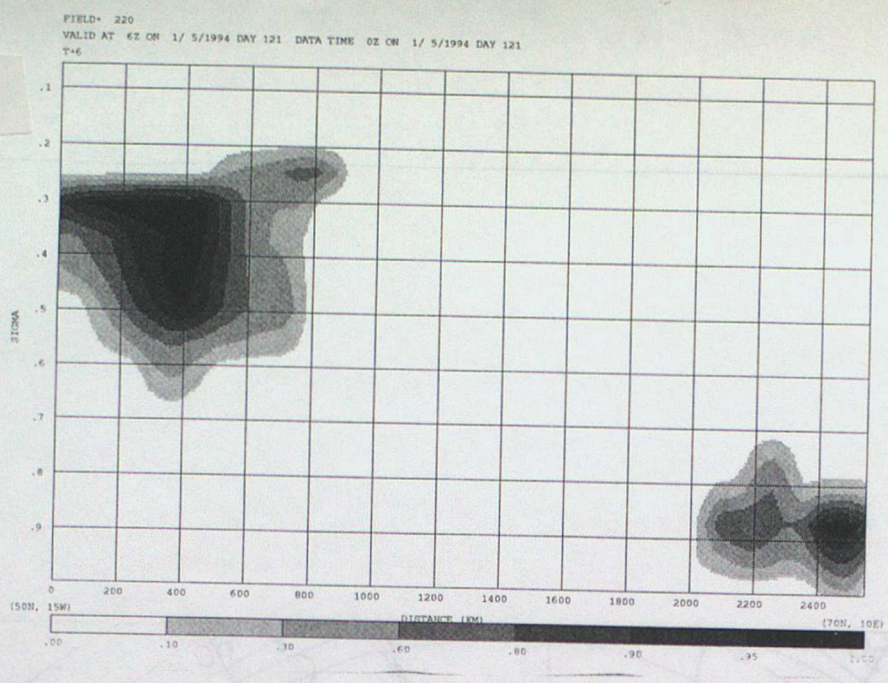

b

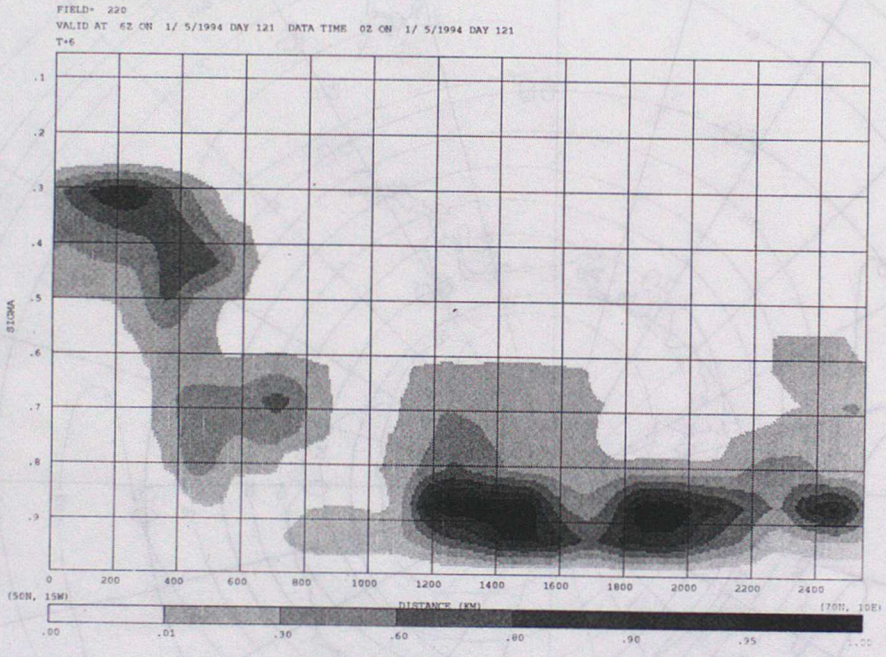

Figure 19a-b
Cross sections showing cloud fraction from 50N 15W to 70N 10E from the Control run and CTT assimilation runs for May 1st 6z.

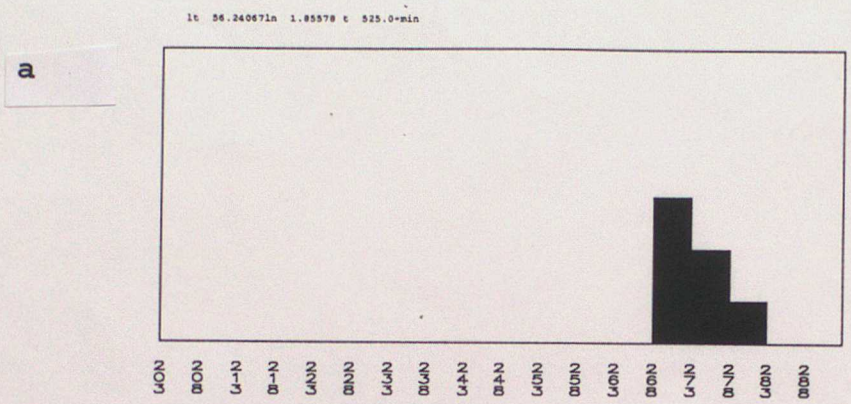

FIELD= 407

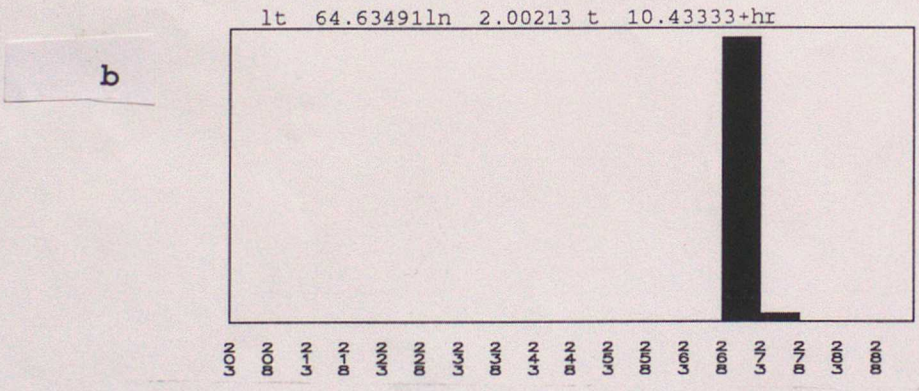

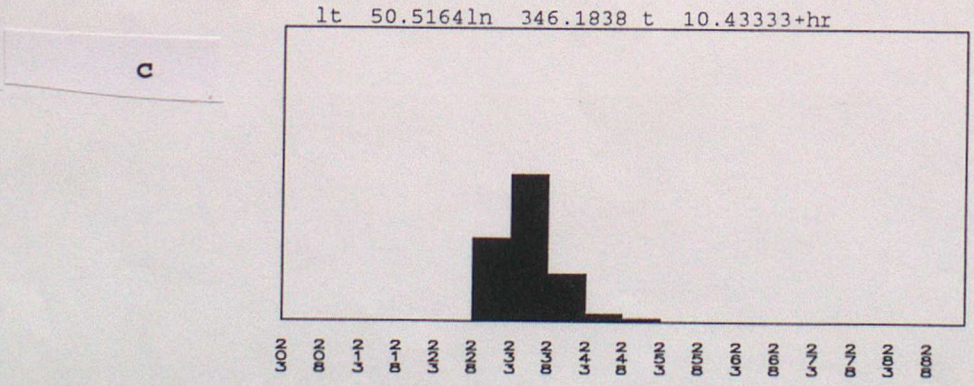

FIELD= 407
VALID AT 0Z ON 1/ 5/1994

Figure 20a-c.
Histograms chosen from the CTT data of the 1 st of May. The lower two correspond to grid boxes along the line of cross section. One to the south western end (the lower histogram) showing the high cold cloud and the middle histogram corresponding to a north sea location showing the lower warmer sea stratus observation.

a

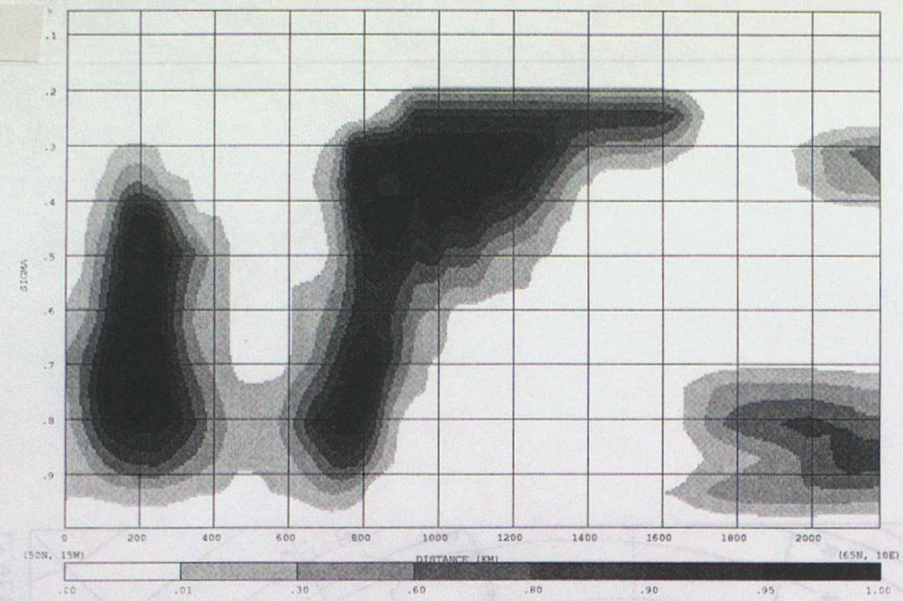

b

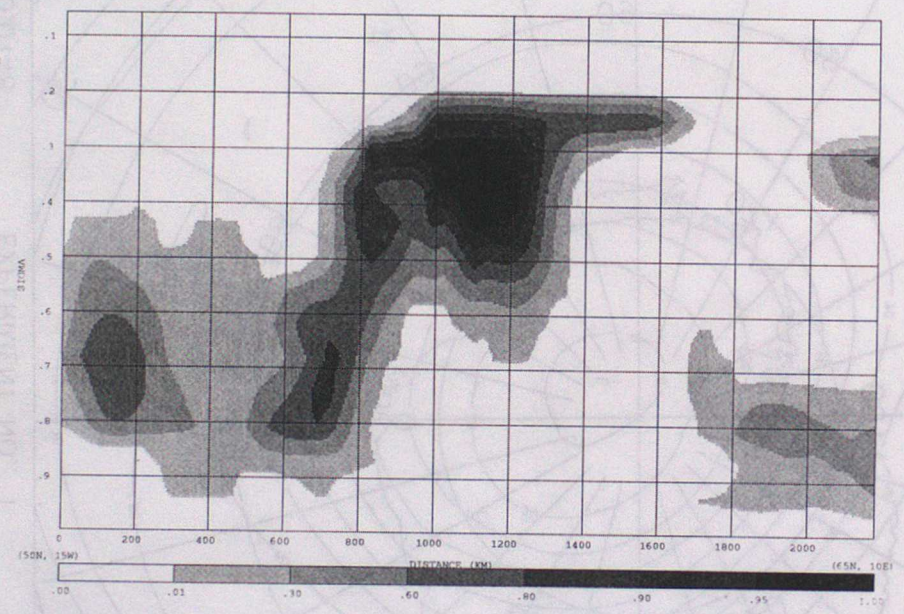

Figure 21a-b

Cross sections showing cloud fraction from 50N 15W to 65N 10E from the Control run and CTT assimilation runs for May 3rd 12Z. The precipitating band shown in the control run and the frontiers data is falling from the cloud approximately 800 km from the left most axis.

a

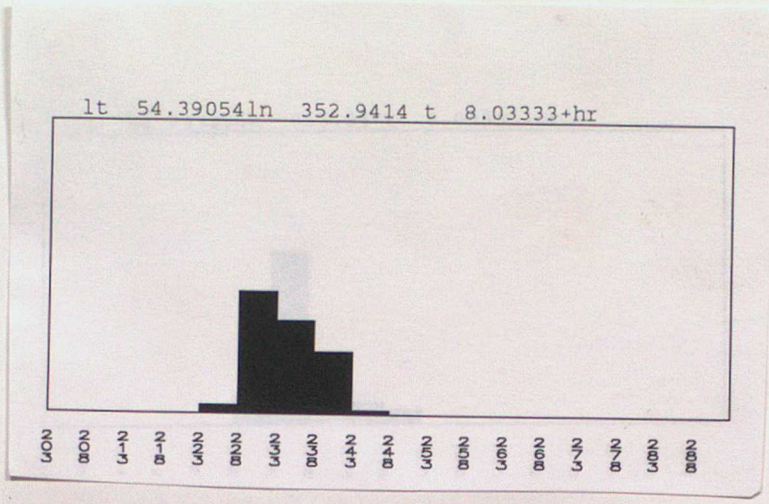

b

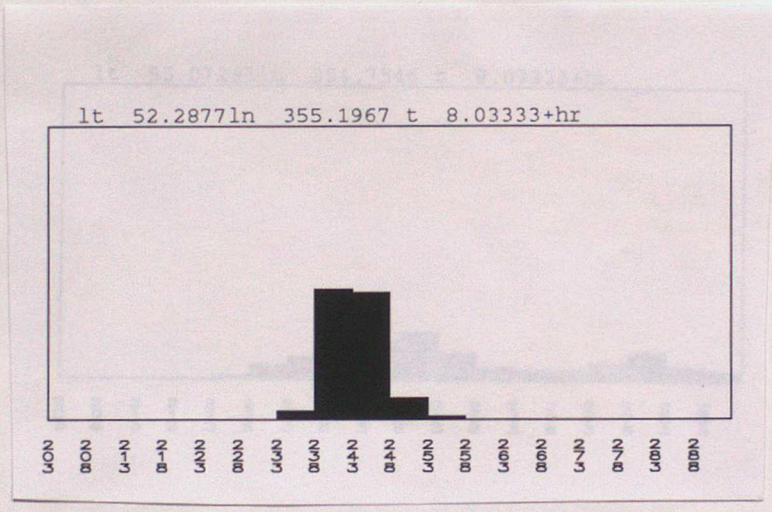

FIELD= 407
VALID AT 0Z ON 3/ 5/1994

c

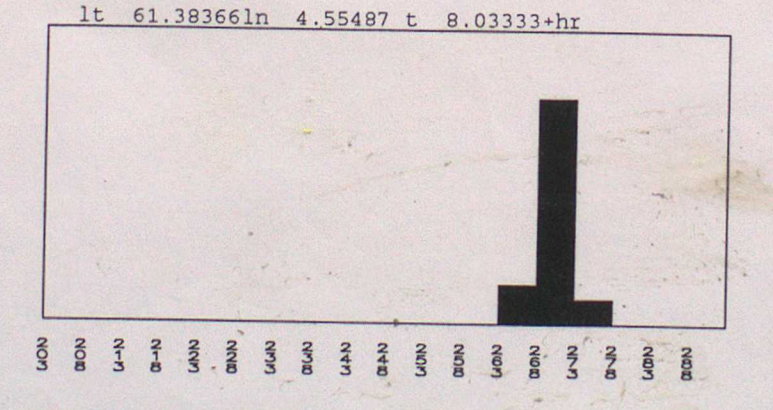

FIELD= 407
VALID AT 0Z ON 3/ 5/1994

Figure 22a-c
Histograms chosen from the CTT data of the 3rd of May. They correspond to observations along the line of cross section shown in figure 14.

VANCLD#2

analysis

a

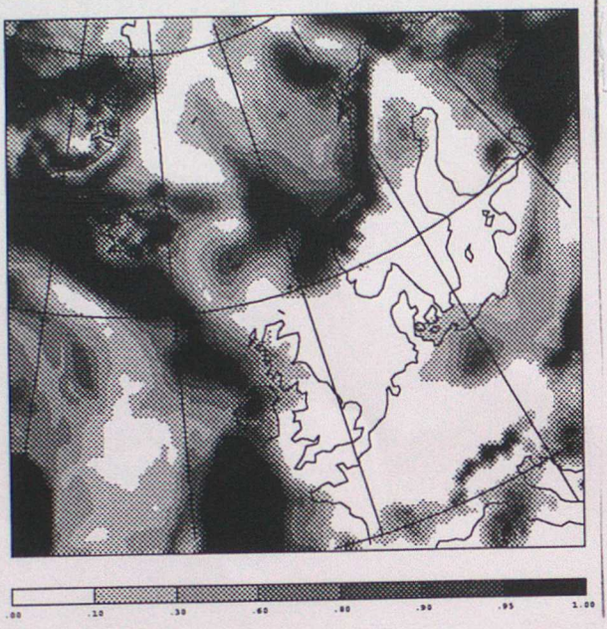

VANCLD#2

12hr forecast

b

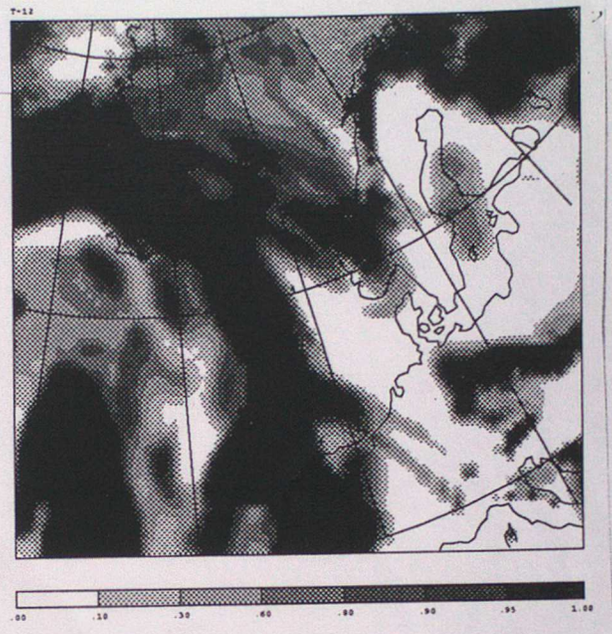

c

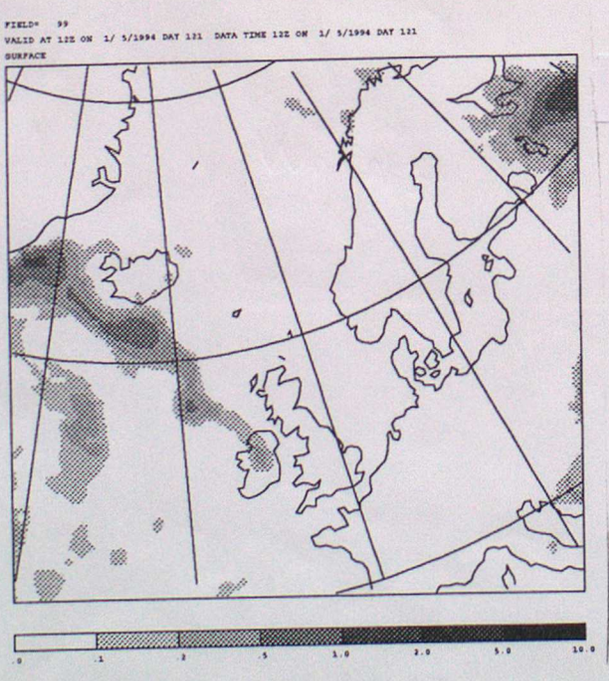

d

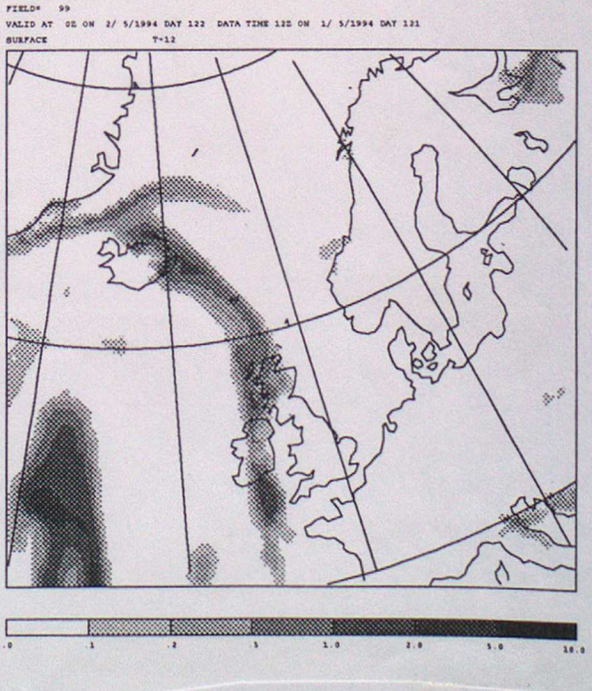

Figure 23a-d
Analysis and forecast cloud and precipitation fields for the 1st of May using VANCLD#2.

control assimilation

VANCLD#2

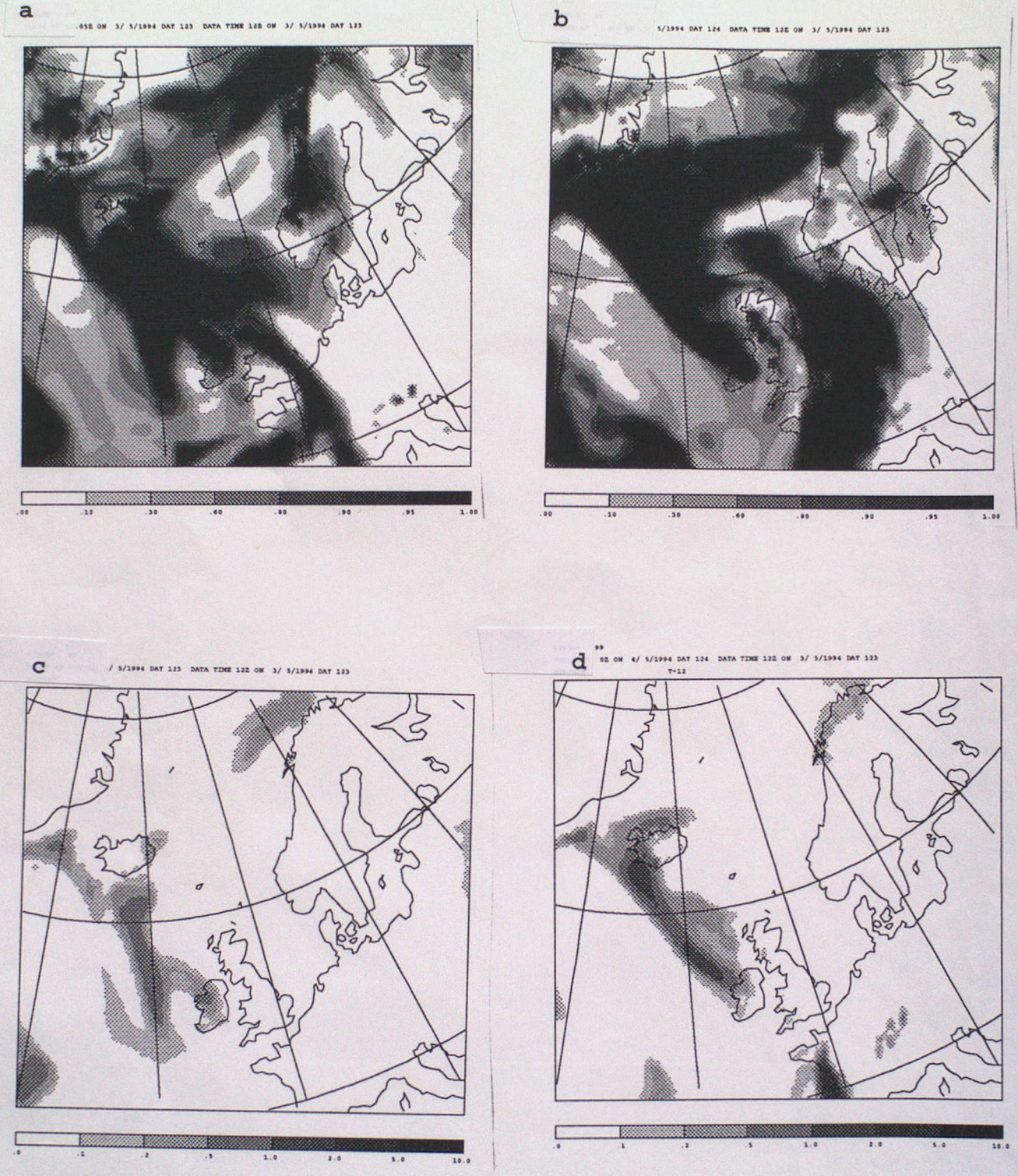

Figure 24a-d
Analysis and forecast cloud and precipitation fields for the 3rd of May using VANCLD#2.

a

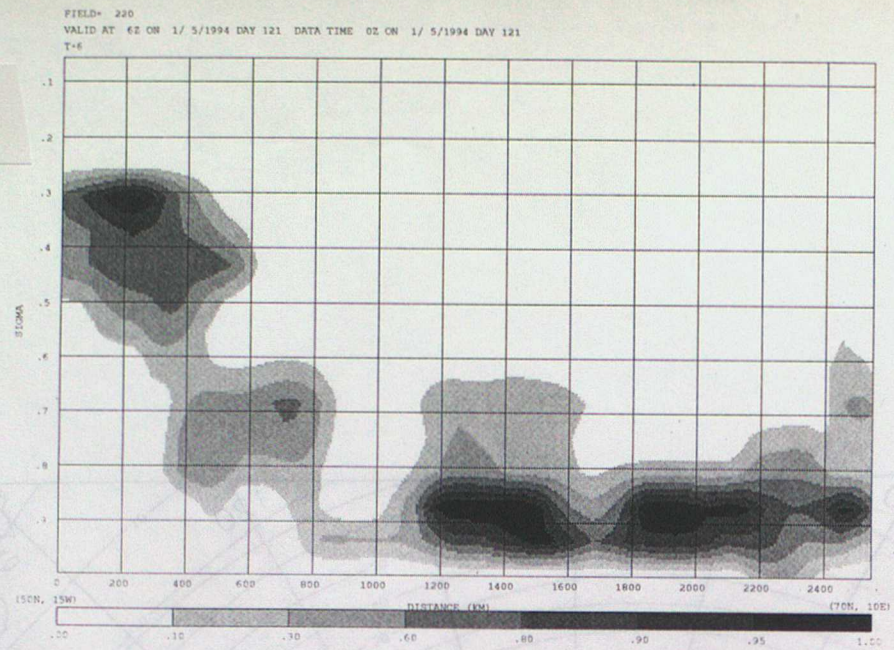

1st May

b

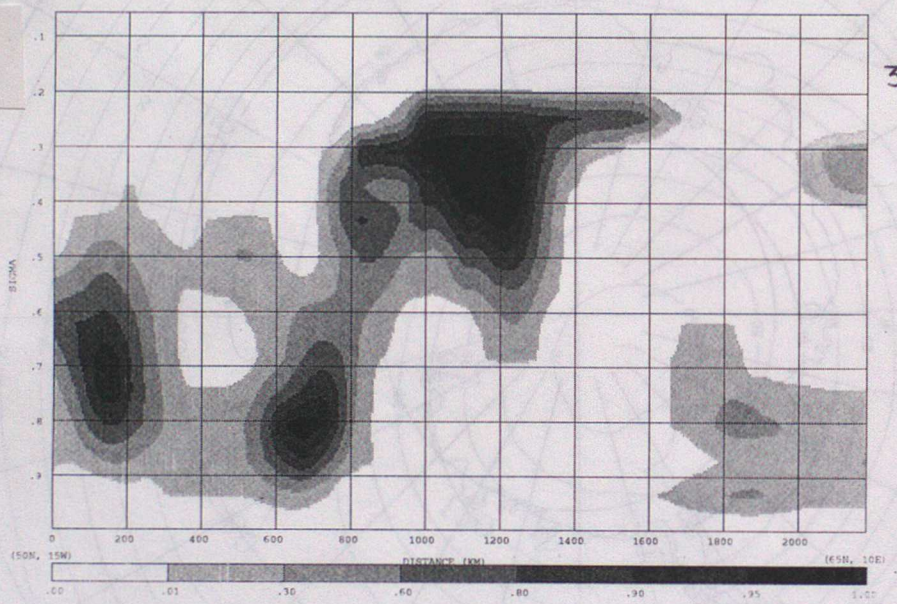

3rd May

Figure 25ab
Cross sections of Cloud fraction for the 1st and 3rd of May using VANCLD#2 CTT assimilation. these charts are comparable with those in figures 12 and 14.

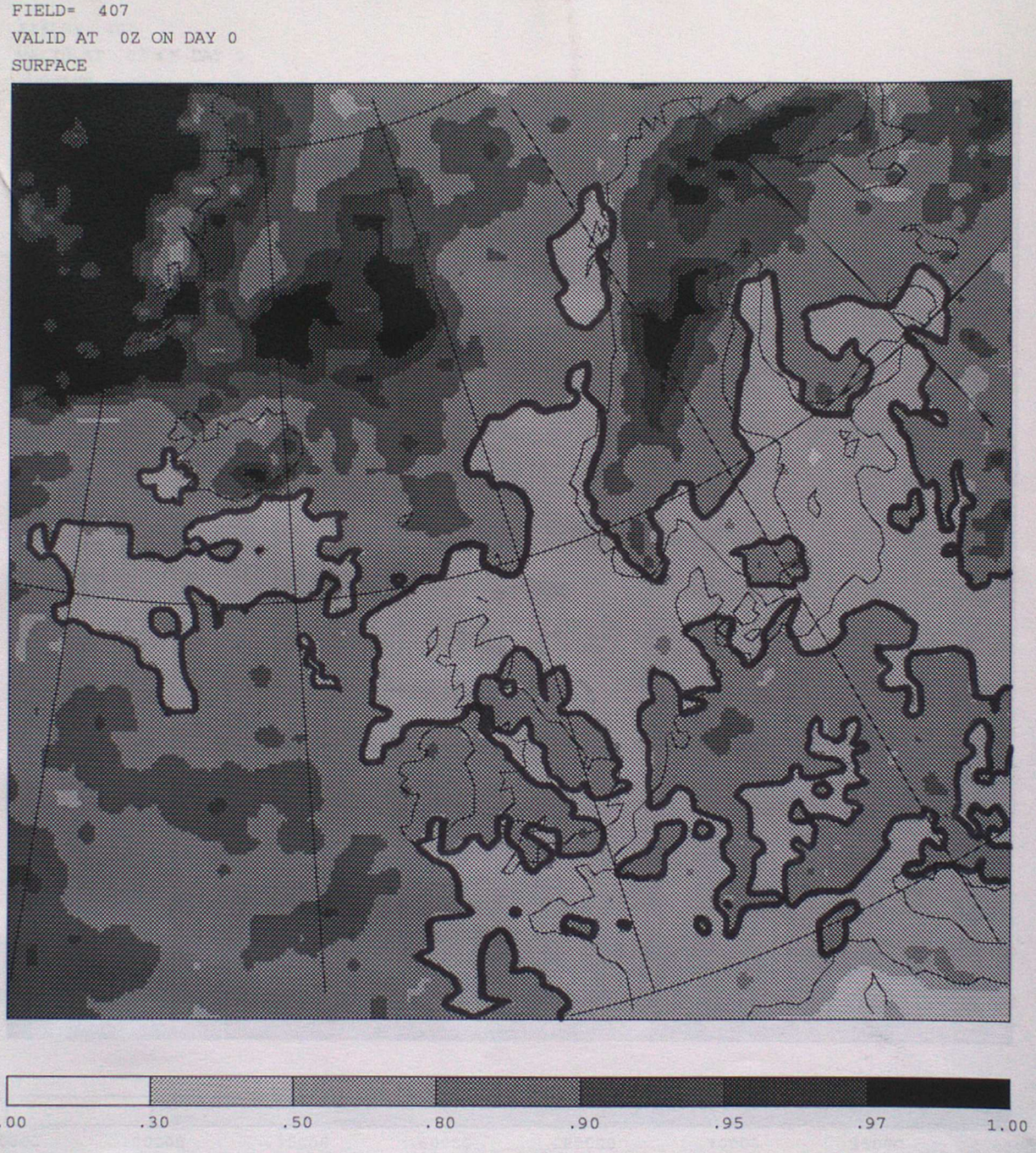

figure B1 total cloud cover averaged for the month of May as calculated from the satellite observations.

figure 32 total cloud cover averaged for the month of May from control model analyses

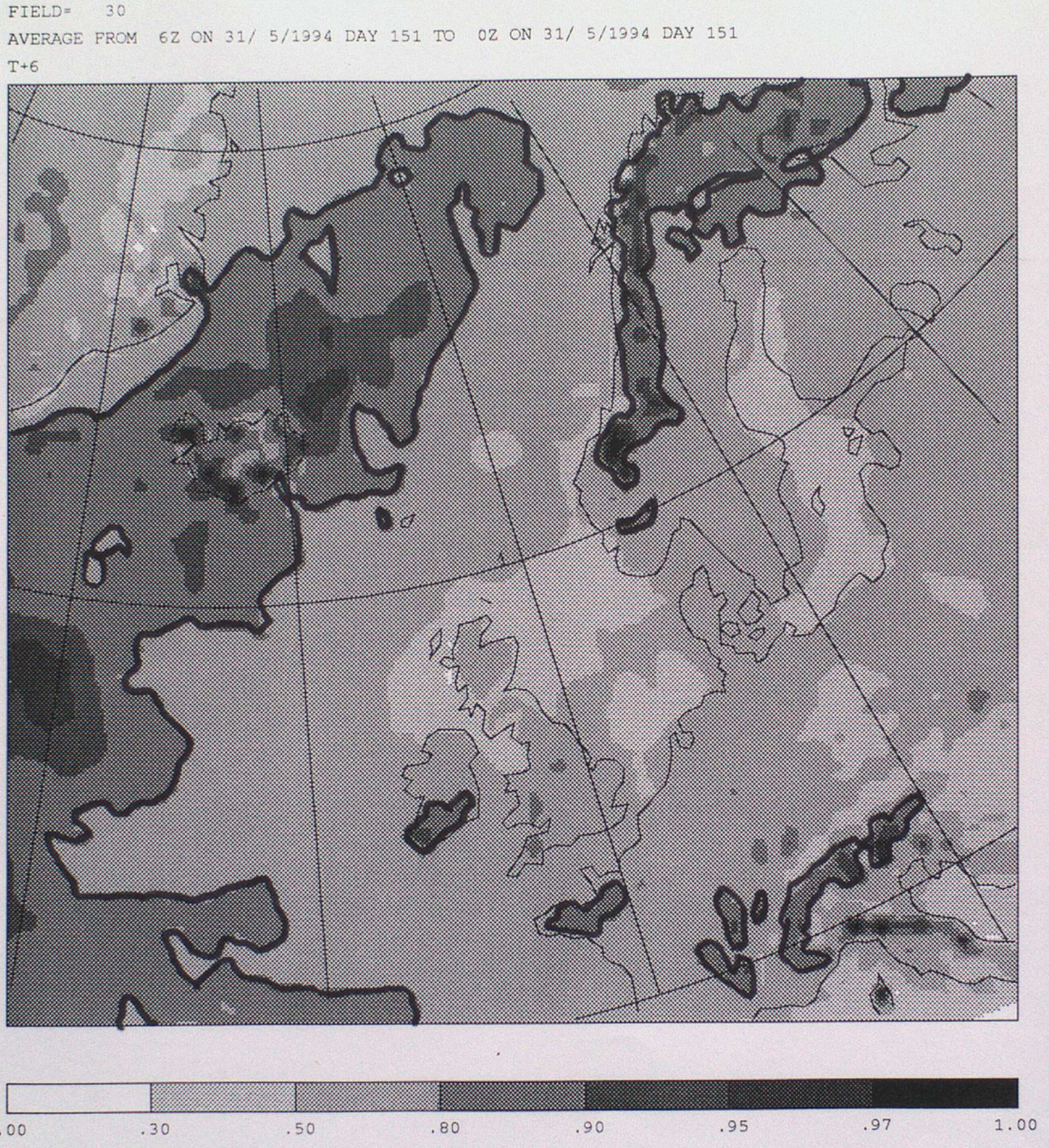

figure 83 total cloud cover averaged for the month of May from CTT assimlation model analyses

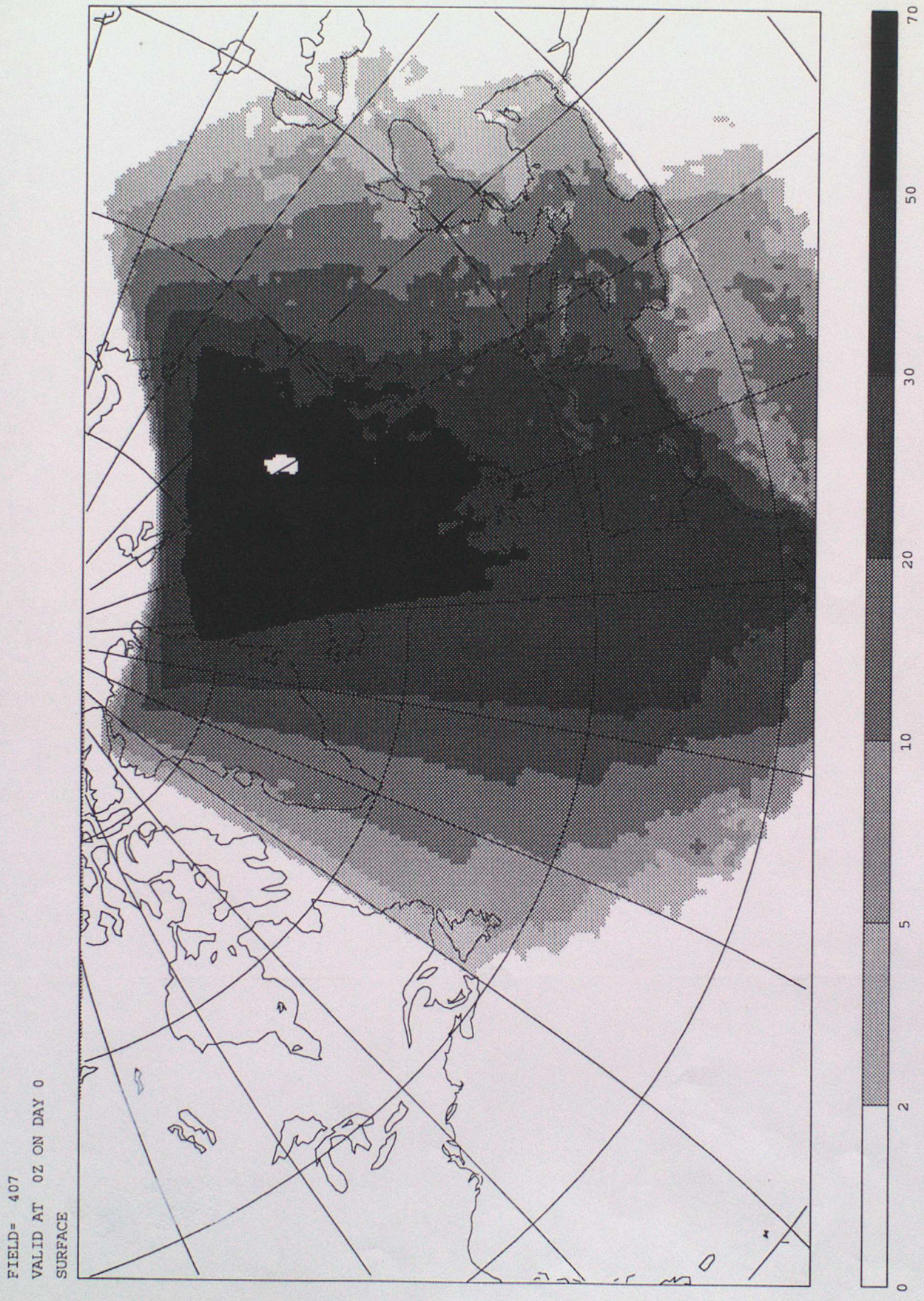

figure B4 total number of satellite CTT observations used in assimilation for each model grid box in May.

FIELD= 30
AVERAGE FROM 6Z ON 31/ 5/1994 DAY 151 TO 0Z ON 31/ 5/1994 DAY 151
T+6

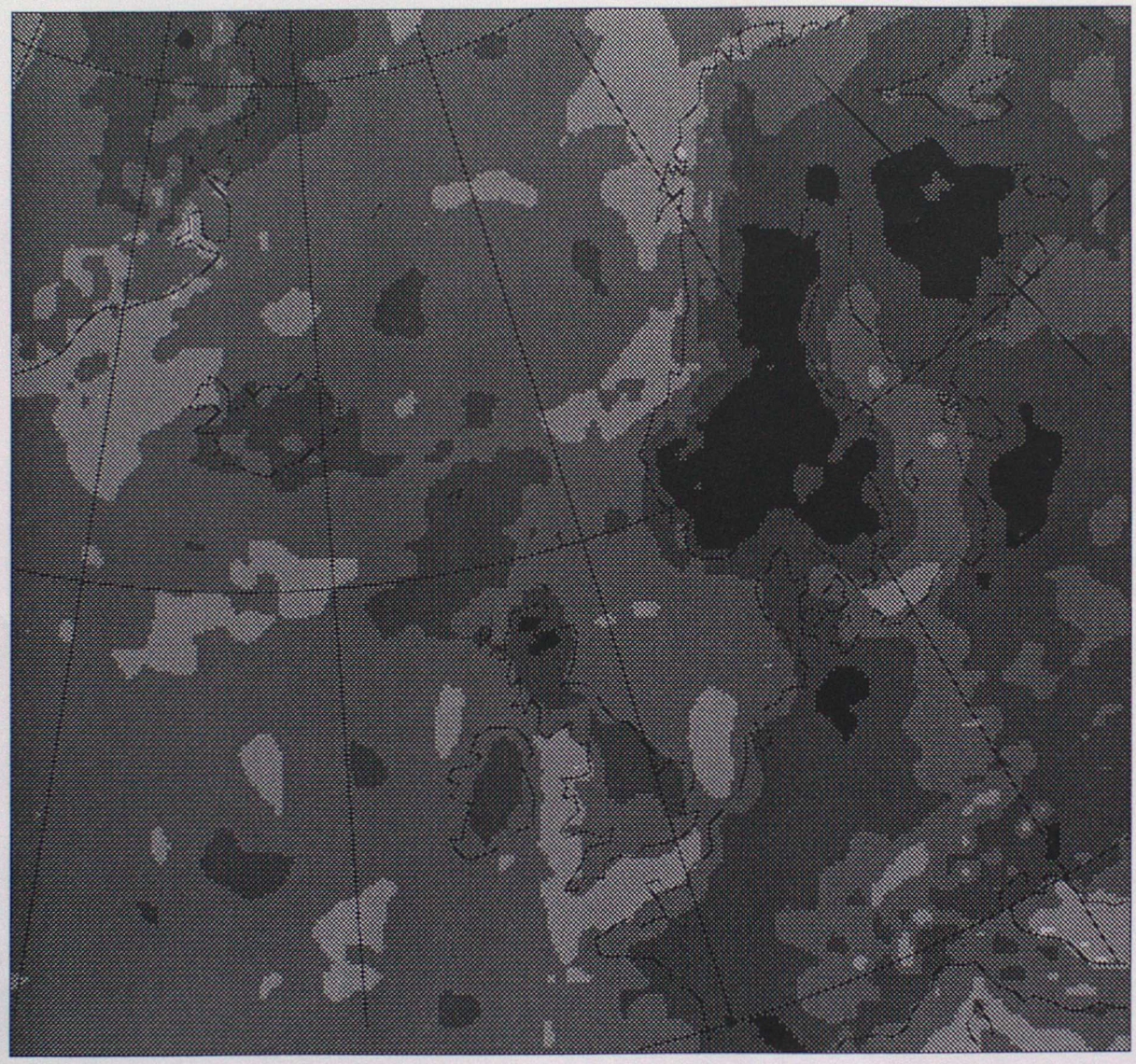

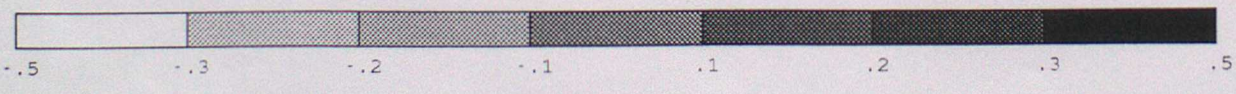

figure 85 difference chart (cloud cover).